Characterisation of High Temperature Stable In-Situ Joints for Grid Cores in C/C-SiC Sandwich Structures

Rahul Shirke

Characterisation of High Temperature Stable In-Situ Joints for Grid Cores in C/C-SiC Sandwich Structures

by

Rahul Shirke

to obtain the degree of Master of Science
at the Delft University of Technology,
to be defended publicly on Thursday February 23, 2017 at 13:30.

Student number:	4408535	
Project duration:	May 9, 2016 – February 22, 2017	
Thesis committee:	Dr. ir. D. Zarouchas,	TU Delft, Supervisor
	Dr. ir. R. Alderliesten,	TU Delft, Committee Chair
	Dr. ir. O. Bergsma,	TU Delft, Assistant Professor
	Dr. ir. J. Fatemi,	TU Delft, External Committee Member
	Ir. B. Heidenreich,	DLR, Supervisor

This thesis is confidential and cannot be made public until February 22, 2022.

TU Delft

Acknowledgement

The path towards this thesis has been circuitous. Its completion is thanks in large part to the special people who challenged, supported and stuck with me along the way. I am grateful to Bernhard Heidenreich for giving me the opportunity to pursue my thesis at DLR-Institute of Structures and Design and guiding me through out the process. I would like to thank Dr.Dimitrios Zarouchas for supporting the project and giving thoughtful feedback which always aimed at moving me forward. Each and every member of Ceramics department of DLR has contributed to the project directly or indirectly. A special thank you to Dr.Otto Bergsma for being the strongest pillar of my support system and for being there whenever I needed help.

I would like to acknowledge the support and motivation given by my colleagues Pranav Kumar and Neraj Jain. I am extremely grateful to my family for their constant understanding, care and support. Finally but most importantly, I would like to thank Sandhya for her love, patience and understanding.

Rahul Shirke
Delft, January 10, 2017

Contents

List of Figures

List of Tables

Abbreviations

ACP Ansys Composite PrepPost

BN Boron Nitride

C/C Carbon/carbon

CMC Ceramic Matrix Composite

CVI Chemical Vapour Infiltration

DIC Digital Image Correlation

LPI Liquid Polymer Infiltration

LSI Liquid Silicon Infiltraion

RTM Resin Transfer Moulding

SEM Scanning Electron Microscopy

SiC Silicon Carbide

Abstract

In the research area of Ceramic Matrix Composites, the development of Carbon/Carbon-Silicon Carbide (C/C-SiC) sandwich structures is a very new topic. The goal of the project is to develop a reproducible manufacturing process for the creation of a C/C-SiC sandwich structure via Liquid Silicon Infiltration (LSI) technique and to optimise the configuration of joining paste used for the adhesion of the skin and the core components of the sandwich structure so that more than 50% SiC is obtained in the joint along with a shear strength greater than 11MPa. A SiC dominant joint avoids oxidation which makes the joint high temperature stable. The potential applications of a C/C-SiC sandwich structure are optical benches in satellites, telescope structures, charging structures for high temperature furnaces, etc. The skin and the core of the sandwich structure are bonded using a joining paste which is converted into a multiphase material consisting of carbon, silicon and silicon carbide (SiC) after siliconisation. The joining paste consists of phenolic or epoxy resin mixed with a carbon particles additive. A sample geometry for tensile test was selected based on the three criteria: Maximum Mean Tensile Strength of the coupons, Minimum Standard Deviation and Uniform distribution of the force on the coupons during the test. The tensile test gave a comparison between the tensile strength of reference phenolic joining paste and epoxy joining paste. Along with the tensile test, elemental morphology of the two joining pastes was also analysed through Scanning Electron Microscopy. It was observed that reference phenolic joining paste is 10MPa stronger than epoxy joining paste and the major reason for the lower strength of epoxy joining paste is the lower carbon content present in the joint. The results from the tensile test were used as a guiding block for the further research performed on shear samples.

For shear test, a sample geometry is selected based on three criteria: similarity to the actual grid core sandwich structure, easy to manufacture without using sophisticated machining techniques and easy to analyse the sample while testing. Based on the data obtained from tensile samples, different variations of phenolic, epoxy and a combination of phenolic and epoxy joining paste is studied. The carbon powder content was systematically reduced by 10% and 20% compared to phenolic joining paste and increased by 50% in epoxy joining paste. An optimum configuration for the mixture of phenolic and epoxy joining paste was determined. The optimum configuration for the phenolic epoxy joining paste was 100:60:120 (phenolic resin: epoxy resin + hardener: carbon powder). In order to avoid gap generated by the manufacturing tolerances of the core, sophisticated and expensive machining techniques like laser and water jet cutting are used. If the gap between the skin and core is not critical then less sophisticated and inexpensive machining techniques can be used for cutting the core component. Hence, the influence of the gap over the shear strength was analysed by manufacturing a shear sample with 0.15mm gap. The maximum gap between the skin and core which the phenolic joining paste could fill was determined by manufacturing a wedge sample. Scanning Electron Microscopy (SEM) analysis provided the information about the elemental composition of the joint which assisted in determining the amount of SiC at the joint and it also helped in observing the effect of the gap on the joint. A shear test similar to ASTM D7078/D7078M-05 was conducted to determine the shear strength of different joining pastes and to assess the effect of the gap on the strength of the joint. Digital Image Correlation technique was used for obtaining the shear strain. Degassing of the resin, using a grooved block with a defined depth so that the thickness of the joining layer is uniform on the core and by using different percentage of silicon uptake for the skin (3mm thick) and the core (0.3mm thick) enhanced the manufacturing process to obtain an uniform distribution of the paste.

The shear coupons failed due to buckling and intra-laminar shear and the failure occurred at the core. Therefore, the strength of the joint could not be determined but a range of core shear stress (23-32 MPa), strain (5-9%) and modulus (0.3-0.4 GPa) was determined. The epoxy joining paste satisfies the goal of obtaining more than 50% SiC in the joint but it also shows low tensile strength and residual stress. Different configurations of phenolic epoxy joining paste can be researched to obtain a SiC dominant joint as the combination of phenolic and epoxy joining paste offers the advantage of room temperature curing which can reduce the manufacturing cost. Another advantage of phenolic epoxy joining paste is that the cured joining paste has low stiffness but after tempering at 210^0C for 2 hours it becomes rigid. This property can open the gates for curved structure applications which can be a boost for the development of CMC structures.

1 *Introduction*

Ceramic Matrix Composites (CMC) are lightweight non-brittle refractory materials which are designed to resist high temperature, high stress and corrosive environment. They are relatively new and still in the developing phase compared to other structural metals and alloys. They are manufactured by using either oxide or non-oxide materials. CMC's have the potential to replace metals and alloys in high temperature applications because of its outstanding properties. Aircraft engine manufacturers like Rolls-Royce and General Electric have initiated their research towards CMC structures so that aircraft engines can be made lighter and fuel efficient. One of the types of CMC which is being studied intensively at German Aerospace Center (DLR) is C/C-SiC. C/C-SiC is a non-oxide type of CMC. C/C-SiC structures offer high temperature stability along with good mechanical strength as shown in Figure 1.1.

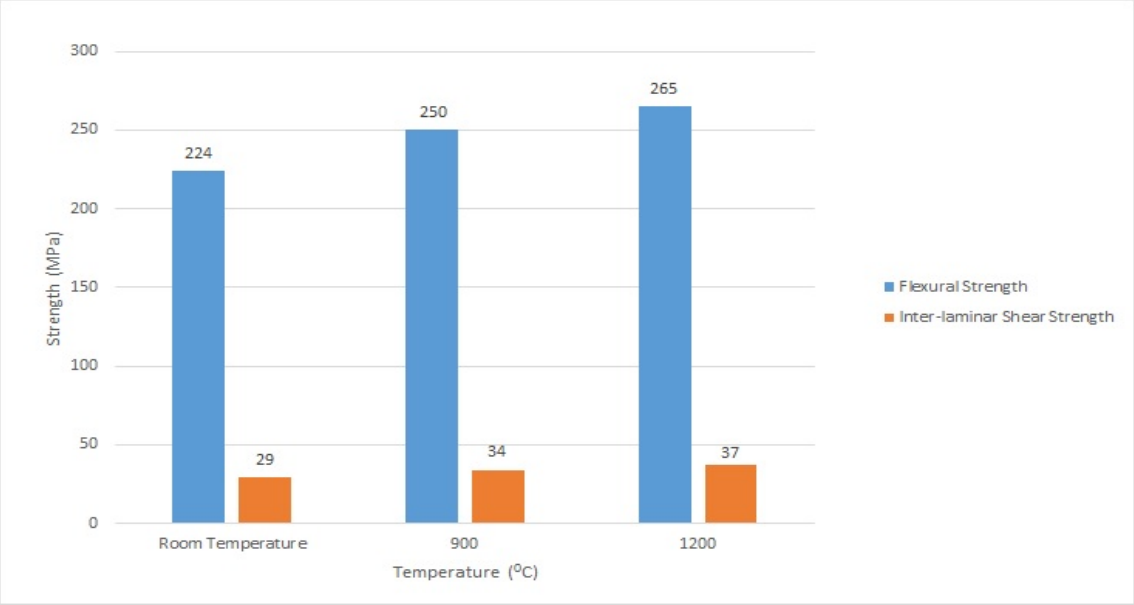

Figure 1.1: High Temperature properties of fabric reinforced C/C-SiC manufactured via LSI [1]

Some of the applications of C/C-SiC structures are nose cap of thermal protection systems, jet vanes in rocket motors, automotive disc brakes, etc [2]. The nose cap of the TPS can withstand a temperature up to 1800^0C and heating rates of several hundred K/s along with high temperature gradient locally which occurs during the re-entry phase of a spacecraft [1]. The nose cap developed for NASA X-38 spacecraft which was considered to be the future crew return vehicle for the International Space Station is shown in figure 1.2. In 2005, a re-entry test flight was conducted with the nose cap made up of flat C/C-SiC panels which could withstand extreme thermal load ($T_{max} > 1727^0C$) at the nose tip as well as the edges of the structure.

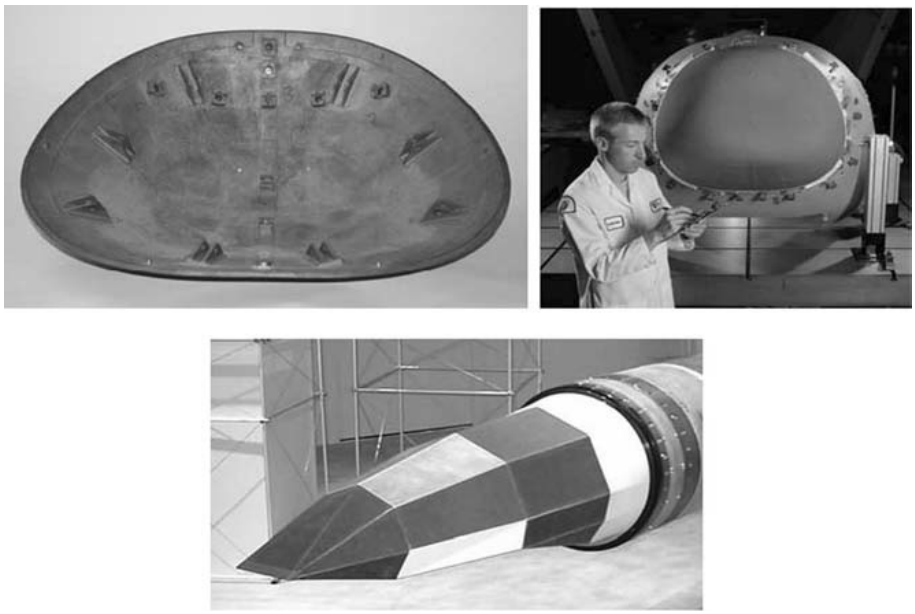

Figure 1.2: C/C-SiC structural parts for TPS. Top left: X-38 nose cap (ca.$740 \times 640 \times 170 mm^3$; t ca. 6 mm; m ca. 7 kg, DLR), showing in-situ joint load bearing elements on the rear side. Top right: Front view of nose cap, mounted on the aluminium structural part of spacecraft. Bottom: Facetted TPS structure, built up by flat panels, mounted on a rocket system.[1]

In short term aeronautics application, jet vanes are used in the thrust vector control systems of the rocket motor where they have to withstand severe thermal and mechanical loads along with a maximum temperature of $2827^0 C$ [2]. Since the service time is short, the oxidation of carbon fibers is not a major problem. The most highlighted advantage of using C/C-SiC jet vanes over metallic (tungsten) jet vanes is the 90% weight saving which is offered by the C/C-SiC material [1]. In long term aeronautics application, C/C-SiC structures cannot be used for replacing the components inside the combustion chamber or turbines because the carbon inside the structure tends to oxidise and degrades the structure. Hence, Si/SiC structures are being researched for gas turbine components.

Currently, grey cast iron is used for the manufacturing of the disc brakes which offer certain disadvantages like corrosion resistance limitation and a high density of $7.3 g/cm^3$. The weight of the disc brake influences the unsprung and rotating mass of the car which in turn affects the agility, handling and performance of the car. The C/C-SiC disc brake overcomes the disadvantages of grey cast iron i.e. the density of a C/C-SiC disc brake is $2.3 g/cm^3$ and it is corrosion resistant. The use of C/C-SiC material offers a weight saving of 50% compared to metallic disc brake and the abrasion resistance property of C/C-SiC extends the service life up to 300,000 km [2]. The serial production of automotive disc brake marks one of the milestones of large scale production of C/C-SiC structures but they are only available in exclusive models of prestigious car brands [2].

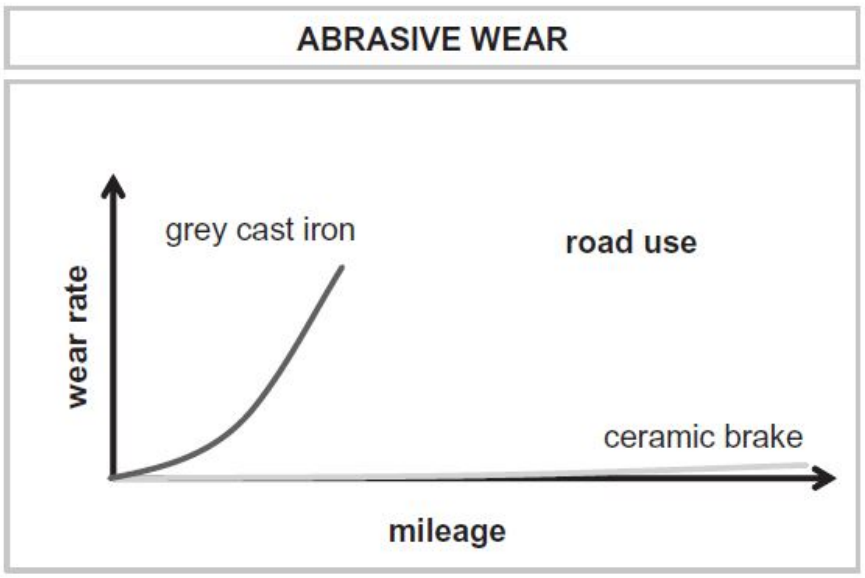

Figure 1.3: Idealized wear behavior of ceramic brake disks under normal braking conditions.[1]

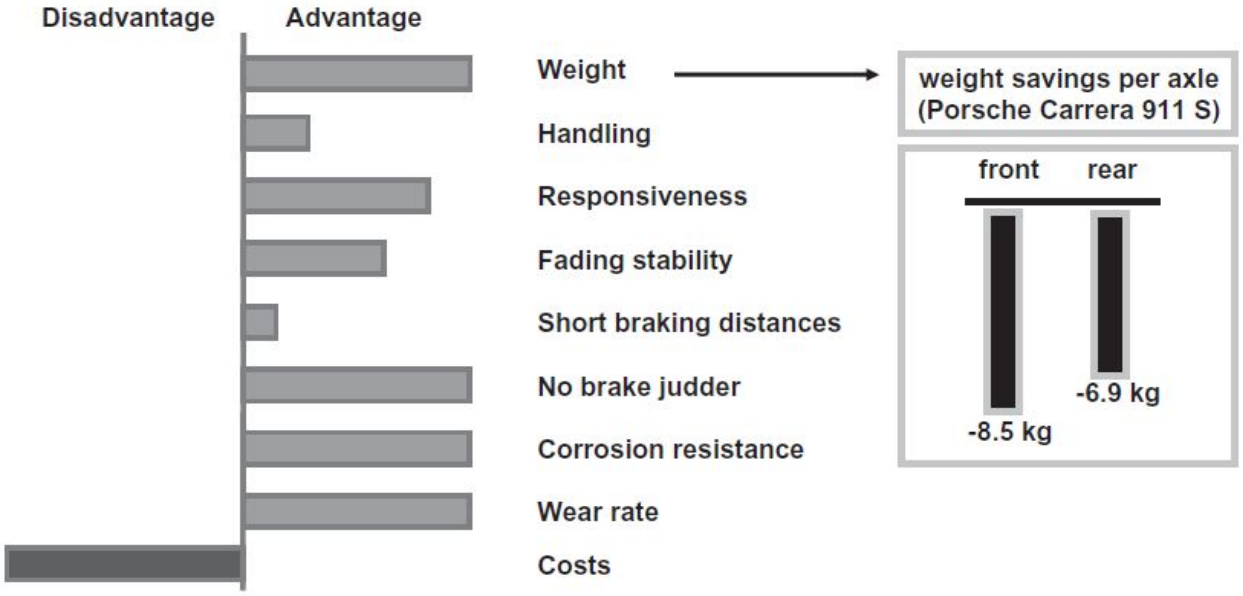

Figure 1.4: Advantages and disadvantages of ceramic brakes compared to grey cast iron disks.[1]

The C/C-SiC composites are developed by using one of the processes mentioned below [3]:

- Chemical Vapour Infiltration (CVI)
- Liquid Polymer Infiltration (LPI)
- Liquid Silicon Infiltration (LSI)

The following descriptions are referred from Ceramic Matrix Composites: Fiber Reinforced Ceramics and their Applications book [3].

In CVI process, each carbon fibre is coated with a thin layer of pyrolithic carbon [2]. After coating, the CFRP is produced by one of the commercial methods and pyrolysed. In order to obtain SiC matrix, the fiber preforms are exposed to a mixture of gas consisting of hydrogen and methyl-trichloro-silan (MTS, CH_3SiCl_3) at a temperature above 800^0C. The chemical reaction which occurs during the infiltration process is shown below:

$$CH_3SiCl_3 \xrightarrow{H_2} SiC + 3HCl$$

Three parameters which should be taken into consideration to ensure a homogeneous SiC deposition are pressure, temperature and volume ratio of hydrogen and MTS. Since the gaseous deposition of silicon does not fill the pores uniformly, (i.e. the pores on the surface gets filled before the inner pores) porosity is increased between 10-15%. The silicon deposition step has to be repeated till desired density is obtained. In LPI process, a slurry is made by mixing a polymer and ceramic powder which is infiltrated into the pyrolithic carbon coated fibres. The shaping and fabrication of the prepreg is carried at low temperature (between 100^0C and 300^0C) via RTM or filament winding process. The pre-ceramic polymer is transformed into ceramic matrix at high temperature ($1100 - 1600^0C$). Thus, after pyrolysis an amorphous or nano-crystalline structure is obtained. Similar to CVI process, the infiltration step has to be repeated several times until the desired density is achieved.

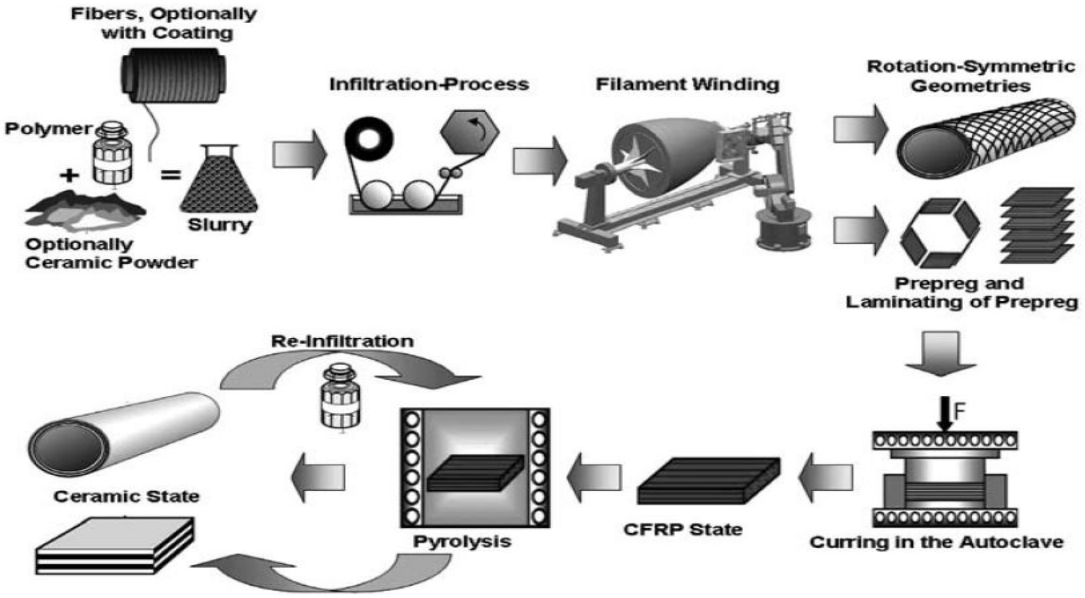

Figure 1.5: Overview of LPI process [1]

For LSI process, the Carbon Fibre Reinforced Polymer (CFRP) preforms are manufactured by using manufacturing techniques like Resin Transfer Molding (RTM), Autoclave Technique or Warm Pressing. Once the 2D (thin walled) Carbon Fibre Reinforced Plastic (CFRP) preforms are manufactured, they are then pyrolyzed at $T > 900^0C$ under inert atmosphere. As a result, the pyrolyisis process gives porous C/C preform. At $T > 1420^0C$ under vacuum condition, the liquid silicon is infiltrated in the porosity with the help of capillary forces. Thus, there is a chemical reaction between Si and C which results in the SiC matrix.

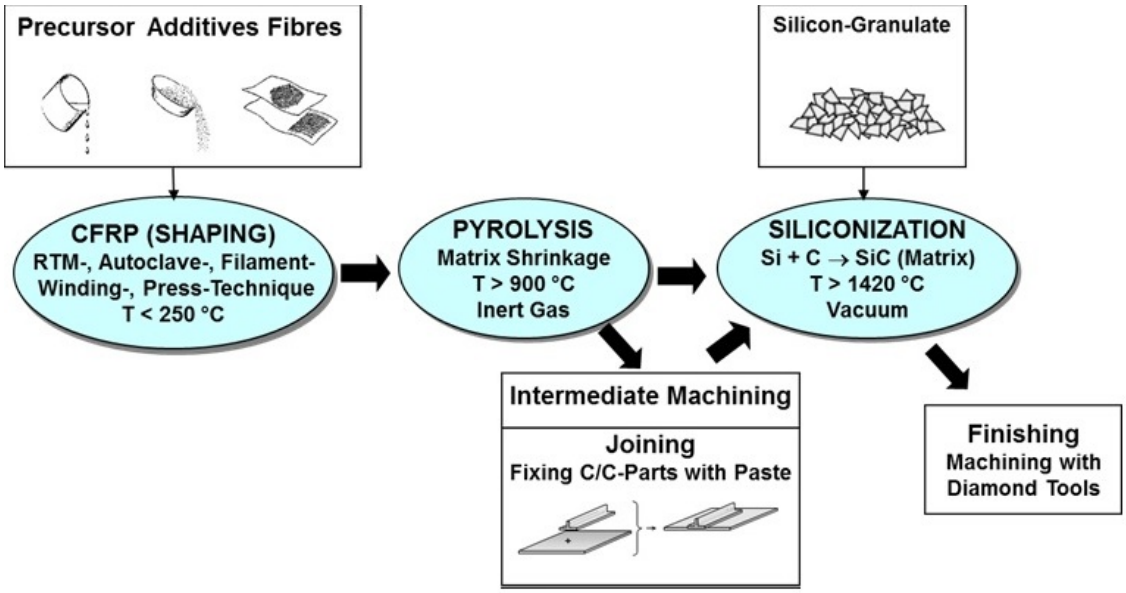

Figure 1.6: Overview of LSI process [1]

Liquid Silicon Infiltration process also offers simplicity in processing by avoiding any fibre coating and re-infiltration steps [1]. Thus, saving the energy required for each re-infiltration step. The average process time for manufacturing a C/C-SiC structure by using LSI technique is 1 week whereas by using CVI or LPI technique it takes more than 3 weeks [3]. Hence, the process time is reduced to a large extent in LSI process which can help in increasing the production of the structure. The LSI process also offers least porosity (2-5%) compared to LPI and CVI process which helps in the improvement of inter-laminar shear strength [2]. All the factors mentioned above makes LSI process a suitable option for producing C/C-SiC sandwich structure.

The major concern for producing a C/C-SiC structure is the manufacturing time and cost, especially for large scale industries. Hence, today, a C/C-SiC structure is considered as a luxury rather than a requirement. For example, an upgrade from metallic disc brake to C/SiC disc brake costs approximately 8000$. DLR-Institute of Structures and Design is trying to bridge this gap by motivating innovative research in the field of CMC's. As a part of the development, this thesis concentrates on improving the joining and integration technology of C/C-SiC structures.

In comparison with the solid metal, composite sandwich structures offer high strength and stiffness to weight ratio due to the thickness offered by the lightweight core material; as shown in Figure 1.7 [4].

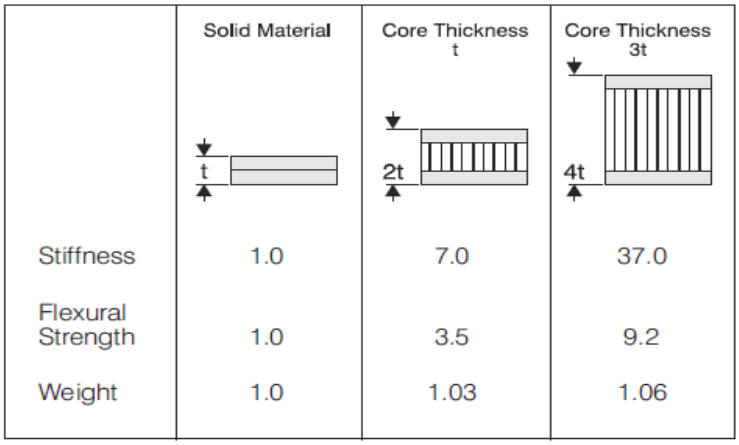

Figure 1.7: Comparison between Solid Metal and Sandwich Panel [5]

Taking a step forward into the research by combining the advantages of composite sandwich structure with high temperature resistance property of C/C-SiC materials, can open the possibilities for the

applications such as lightweight optical benches in satellites, charging structures for high temperature furnace or telescope structures. Hence, filigree core structures with high mechanical load capacity are needed.

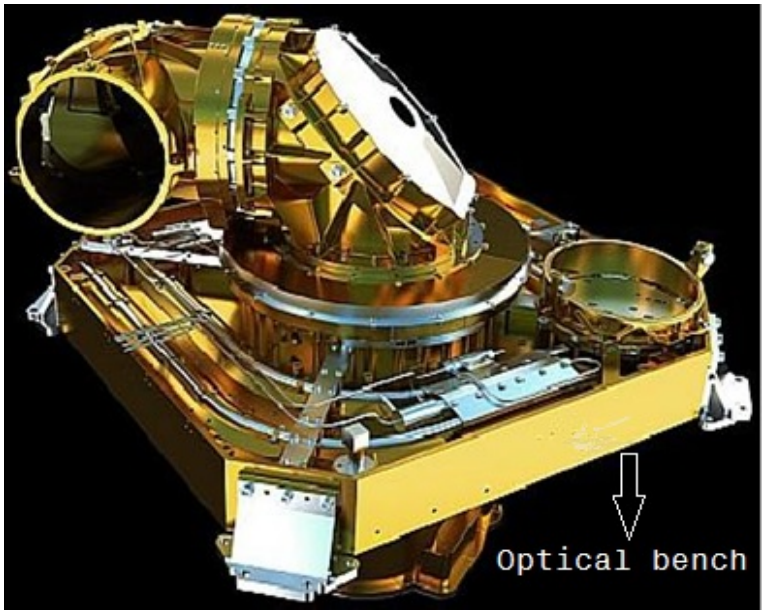

Figure 1.8: FUS (Frame Unit Structure) in LCT-Project (ESA).

At DLR, the effect of different core geometries is studied for developing C/C-SiC sandwich structures by using LSI process [6] [7]. The grid core as shown in Figure 1.9 is one of the core geometries which is being researched for the C/C-SiC sandwich structures.

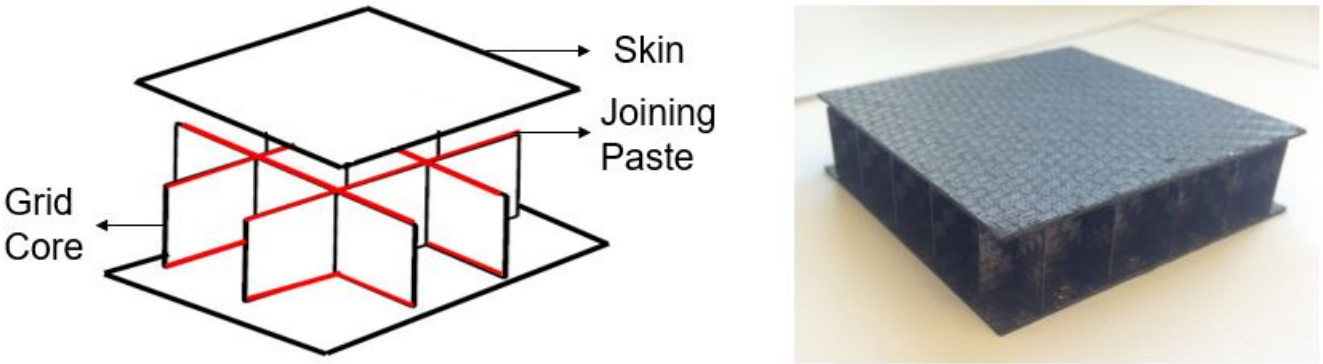

Figure 1.9: C/C-SiC Grid Core Sandwich Structure

In manufacturing C/C-SiC sandwich structure via LSI process, the C/C grid core is fixed to the C/C skin with the help of a polymer joining paste [8]. The schematic representation of the joining step is shown in figure 1.6. Once the joining paste is cured then the whole structure is put through siliconisation. The joining paste ensures that the structure is temporarily bonded but the final joining happens only after the infiltration of silicon. After the siliconisation, the carbon in the joining paste gets chemically transformed to SiC. Along with SiC, the elements which are expected inside the joint are residual carbon and silicon. The proportion of these elements depend upon the type of resin, amount of additive and amount of silicon infiltrated. If the joint has more than 50% residual carbon then it loses the ability to withstand high temperature due to the oxidising nature of carbon at high temperature and excess Si makes the joint brittle. Therefore, a SiC dominant joint i.e. more than 50% SiC is required to achieve thermal stability at high temperature (above 1500^0C). According to previous research on C/C-SiC joint, the shear strength of phenolic resin was determined to be 11MPa at room temperature. Thus, considering 11MPa as reference shear strength.

The main focus of this research is to obtain a homogeneous distribution of the joining paste with more than 50% SiC content at the joint and a shear strength greater than 11MPa [8][7]. Since the configuration of the joining paste and the joining method influences the final joint, various combinations of joining paste are researched to obtain the optimum joining paste and joining method is refined to obtain a homogeneous distribution of the joining layer.

1.1 Research questions, aims and objective

The main aim of this work is to characterise the joining paste which is used for the adhesion of the skin and the core components of the sandwich structure and to develop a reproducible manufacturing technique for the development of C/C-SiC sandwich structures with grid cores.

1. How to improve the joining of C/C-SiC grid core sandwich structure manufactured by using LSI technique?
   (a) How can the existing LSI manufacturing procedure be improved with respect to the reproducibility?
   (b) How to determine tensile strength of the joint?
   (c) What parameters of the joining paste can be varied to give more than 50% SiC at the joint and a shear strength greater than 11 MPa?
   (d) How does the gap between the skin and the core component influences the shear strength of the joint?
      i. How to determine the maximum gap between the skin and the core component?
2. How to determine the shear strain in a thin walled C/C-SiC structure?

1.2 Overview of Chapters

- State of the Art.
- Methodology.
  - Grid Core Dimensions
  - Tensile Test Sample - Sample Geometry, Joining Paste, Manufacturing Procedure, Results and Elemental Morphology. The results from tensile test are referred for shear test analysis.
  - Shear Test Sample - Sample Geometry, Experimental Setup, Digital Image Correlation (ARAMIS), Scanning Electron Microscopy.
- Variation of Joining Paste.
- Gap Analysis.
- Results and Discussion - ARAMIS reproducibility and reliability proof, Shear Test and Elemental Morphology.
- Conclusion and Recommendation.

2 *State of the Art*

The literature mentioned below is referred from Ceramic Matrix Composites: Fiber Reinforced Ceramics and their Applications book [3]. The manufacturing of large CMC components and complex geometries becomes challenging with the existing manufacturing techniques. Joining of smaller components with simpler geometries makes the task easier. Hence, there has been a great motivation towards studying the joining and integration of CMC components. The common techniques used for joining CMC are diffusion bonding, adhesive bonding, active metal brazing and reaction forming.

For joining dissimilar materials like ceramic to metal, active metal brazing technique is used. The advantages of this technique is its simplicity and cost effectiveness. However, the joint can only withstand moderate temperatures.

At NASA Glenn Research Center, a robust joining technology know as ARCJoinT is developed for bonding C/C-SiC structures.

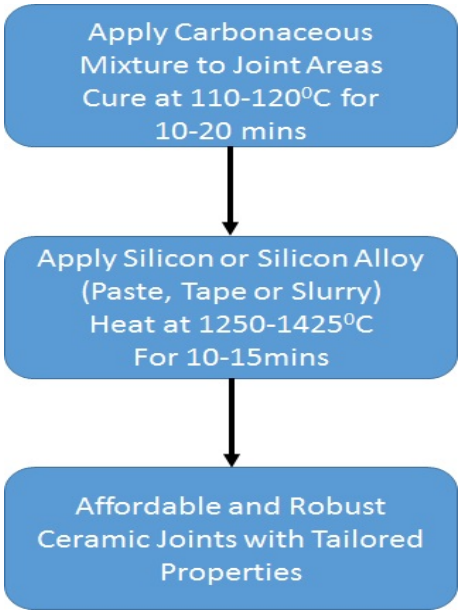

Figure 2.1: Flow diagram of ARCJoinT ceramic joining technology developed at NASA GRC [3]

The silicon or silicon alloy chemically react with carbonaceous mixture to form SiC which makes the joint thermally stable at high temperatures by avoiding oxidation. If silicon alloy is used for example Si-Ti then other phases ($TiSi_2$) are also formed. It was also observed that the shear strength of the C/SiC joint manufactured using ARCJoinT technique was more than the shear strength of C/SiC composite at elevated temperature up to 1350^0C.

A double notch compression test i.e. ASTM C 1292-95a was conducted on C/SiC composite joint manufactured using CVI and ARCJoinT technique. The test setup failed to induce pure shear as both shear and normal compression stresses were generated. It was observed that the shear strength of the joint increased with the increase in temperature. The reason for the increase in shear strength is the release of residual stresses which were generated during the manufacturing process.

The techniques used for joining of CMC components can be used for repairing CMC structures. NASA Glenn Research Center has developed a new material known as Glenn Refractory Adhesive for Bonding and Exterior Repair (GRABER) which can be used to repair C/C composite thermal protection systems in shuttles. The unique property of the material is that it does not require post processing and it converts to high temperature stable ceramic during re-entry conditions. A test was conducted under re-entry condition on a C/C composite structure which was repaired with GRABER. The test was conducted for 15mins and it was observed that the repaired area did not allow the transmission of hot plasma and other gases through the structure.

Currently, LPI and CVI are the commercially used manufacturing techniques for the production of C/C-SiC structures. According to the patent on Ceramic honeycomb structures and method, the honeycomb core structure is manufactured using CVI process. The manufacturing procedure is as

follows [9]:

1. A prepreg consisting of fabric and binder is loosely woven into a honeycomb shape. The fabric usually used is metallic, ceramic or organic fibers and the binder used is either made up of organic or inorganic materials. It should be noted that only organic binder should be used with metallic or ceramic fabric.

2. The woven honeycomb is pyrolysed between 700^0C to 1100^0C. During pyrolysis, the honeycomb structure becomes porous as the binder gets evaporated but the geometry of the structure is retained.

3. The silicon matrix is formed by the chemical reaction of trichloromethylsilane and hydrogen on the porous carbon-carbon honeycomb. Thus, a C/SiC honeycomb core is manufactured.

4. The C/SiC skins are manufactured separately and bonded to the C/SiC honeycomb core with ceramic adhesive.

Another research study was made on C/SiC sandwich structure with stitched lattice core. The manufacturing procedure is explained below **lattice**

1. Woven carbon-fabric cloth is infiltrated with polycarbosilane which forms the top and the bottom skin of the C/SiC sandwich structure.

2. Holes are drilled on the top and bottom skins. The towpreg is stitched from the bottom skin to the top skin.

3. The stitching is completed when the desired lattice configuration is obtained.

4. After stitching the lattice core, the structure is vacuum bagged and cured in autoclave under 0.3 MPa at 120^0C for 180 min and then 150^0C for 180 min. Since the lattice core is not coated with any ceramic, the structure cannot be used for high temperature applications.

Figure 2.2: C/SiC composite sandwich structure with stitched lattice core **lattice**

In the journal "The preparation and performance of a novel room-temperature-cured heat-resistant adhesive for ceramic bonding," adhesive used for joining two ceramic structures is produced by using silicon–epoxy interpenetrating polymer networks (IPNs) as matrix (based on silicon resin (SR) and diglycidyl ether of bisphenol A (DGEBA) epoxy resin (EP), γ-glycidoxypropyltrimethoxysilane (γ-GPS) as cross-linking agent, dibutyltin dilaurate (DBTDL) as catalyst, Al, low melting point glass (GP) and B4C powders as inorganic fillers, low molecular polyamide (LMPA 650) as curing agent **ro0m** Due to the use of epoxy resin, the adhesive has an advantage of room temperature curing and the highest temperature which the joint can withstand is 1000^0C. Another adhesive which can be used for bonding the SiC ceramic material is developed by modifying polymethylsilane with D4Vi [10]. It can withstand up to 1200^0C. Both the adhesives cannot be used for LSI process as the siliconisation cycle reaches a temperature of 1600^0C.

Although CVI process is widely used, it has some drawbacks with respect to achieving complete densification of large and complex geometries and long process time. LPI process has disadvantages of multiple re-infiltration and pyrolysis cycle which in turn increases the cost of manufacturing. LSI process overcomes the disadvantages of CVI and LPI process. LSI process gives the least porosity in the end product, it has only one silicon infiltration cycle and it has the shortest process time compared to the other two processes. Hence, LSI process is selected to study the joining of C/C-SiC grid core sandwich structures. According to the authors best knowledge, there is no existing literature on C/C-SiC sandwich structures manufactured via LSI process.

At DLR, another C/C-SiC joining technique is developed by Walter Krenkel. The C/C components are joined with a carbonaceous binding material mixed wih JK60 phenolic resin. JK60 was also used as a precursor matrix in the manufacturing of CFRP plates which are pyrolysed to obtain C/C plates. The joining paste is cured at 135^0C for 1.5 hours and then the whole structure is siliconised. The carbon inside the joint is chemically transformed to SiC. The siliconisation of the structure and the joining takes place in a single cycle which reduces the process time. Three types of bonding materials were tested :

1. Only joining paste
2. Fabric with joining paste
3. Felt with joining paste

Three combinations of specimens were also studied. The three combinations are:

1. grounded specimens
2. ungrounded specimens
3. combination of grounded and ungrounded specimens

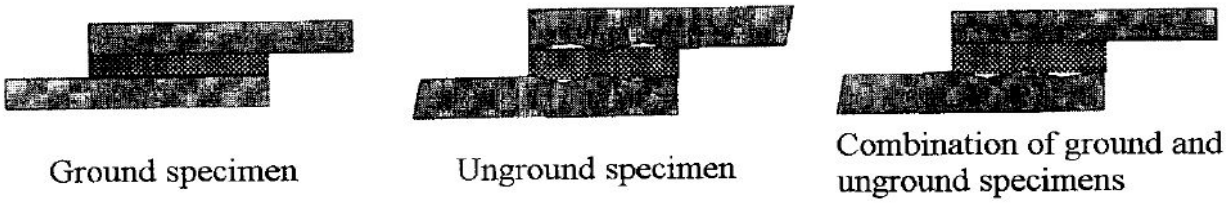

Figure 2.3: Combinations of the spceimens [8]

The shear test results for each combination is showed in figure 2.4.

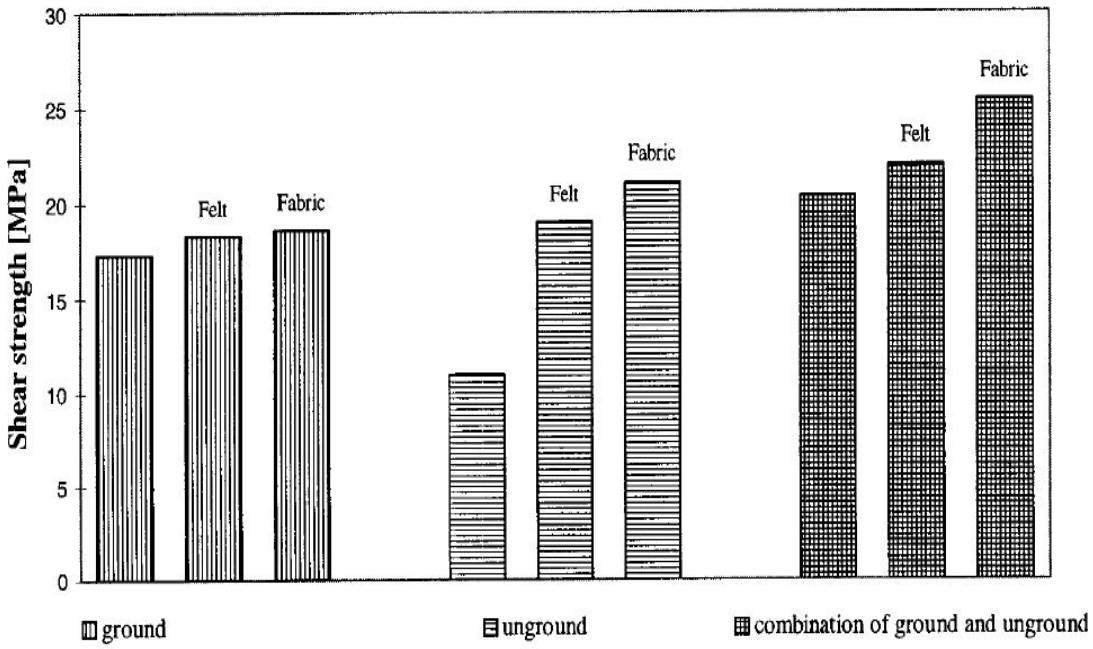

Figure 2.4: Combinations of the spceimens [8]

In all the combinations, the lowest shear strength was obtained for the samples only with joining paste. It was observed that the use of felt or fabric with the joining paste increased the shear strength of the joint. This is due to the uniform distribution of the paste through the fabric or felt. A significant increase in shear strength value of fabric and felt combination compared to only paste was observed in the ungrounded specimen. The steep increase in shear strength is because the fabric and felt accommodate to the contours of the ungrounded specimen which results in uniform and stronger joint.

The journal "In-Situ Joined CMC Components" is considered as the main reference for this thesis work. The joining methodology and technique is applied for manufacturing C/C-SiC grid core sandwich structure via LSI process.

The figure 2.5 shows the comparison between the material properties of C/SiC and C/C-SiC manufactured by using CVI, LPI and LSI process.

			CVI		LPI	LSI		
			C/SiC	C/SiC	C/SiC	C/C-SiC	C/C-SiC	C/SiC
Manufacturer			SPS (SNECMA)	MT Aerospace	EADS	DLR	SKT	SGL (9)
Density		g/cm³	2.1	2.1 - 2.2	1.8	1.9 - 2.0	> 1.8	2 / 2.4
Porosity		%	10	10 - 15	10	2 - 5	-	2 / <1
Tensile strength		MPa	350	300 - 320	250	80 - 190	-	110 / 20-30
Strain to failure		%	0.9	0.6 - 0.9	0.5	0.15 - 0.35	0.23-0.3	0.3
Young's modulus		GPa	90 - 100	90 - 100	65	50 - 70	-	65 /20-30
Compression strength		MPa	580 - 700	450 - 550	590	210 - 320	-	470 / 250
Flexural strength		MPa	500 - 700	450 - 500	500	160 - 300	130 - 240	190 / 50
ILSS		MPa	35	45 - 48	10	28 - 33	14 - 20	-
Fibre content		Vol.%	45	42 - 47	46	55 - 65	-	-
CTE Coefficient of thermal expansion	∥	10^{-6} K^{-1}	3(1)	3	1.16(4)	-1 - 2.5(2)	0.8-1.5(4)	-0.3 / 1.8 (5)
	⊥		5(1)	5	4.06(4)	2.5 - 7(2)	5.5-6.5(4)	-0.03–1.36 (6) / 3 (7)
Thermal conductivity	∥	W/mK	14.3-20.6(1)	14	11.3-12.6(2)	17.0-22.6(3)	12 - 22	23–12 (8) / 40-20 (8)
	⊥		6.5 - 5.9(1)	7	5.3 - 5.5(2)	7.5 - 10.3(3)	28 - 35	
Specific heat		J/kgK	620 - 1400	-	900-1600(2)	690 - 1550	-	-

∥ and ⊥ = Fibre orientation: (1) RT - 1000 °C ; (2) RT - 1500 °C; (3) 200 - 1650 °C; (4) = RT - 700 °C; (5) 1200 °C; (6) 200 – 1200 °C; (7) 300 – 1200 °C; (8) 20 °C – 1200 °C; (9) values for fabric/short fibre reinforced material

Figure 2.5: Typical material properties of C/SiC and C/C-SiC materials in dependence of the manufacturing method[2]

A summary on shear strength of C/C, C/SiC and Si/SiC composite joints shown in figure2.6.

Joined materials and surface preparation	Joint materials	Temp. (°C)	Strength (MPa)	Comments
C/C composite system	Rheocast Cu-Pb alloy	25	1.5	Strength of Cu/Cu joint with Cu-Pb alloy: 3 MPa at 25 °C
C/C-SiC composite system[a]	Carbon paste Carbon felt Carbon fabric	25 25 25	17 18 18.5	Minor improvement in strength, some porosity and free Si
C/C-SiC composite system[b]	Carbon paste Carbon felt Carbon fabric	25 25 25	11 19 21	Significant increase in joint strength
C/C-SiC composite system[c]	Carbon paste Carbon felt Carbon fabric	25 25 25	21 22 26	No porosity or free Si in the joint region
C/C-SiC composite system	Liquid Si infiltration of a carbon paste applied to the joint with or without C fabric	25 25	21.5 ± 2.28 113–198[d]	
CVI SiC/SiC composite system	ARCJoinT (carbonaceous mixture at the joint, cure, infiltrate with Si or Si alloys)	25 800 1200	65 ± 5 66 ± 9 59 ± 7	4-point bend test
MI Hi-Nicalon/BN/SiC composite system	ARCJoinT (carbonaceous mixture at the joint, cure, infiltrate with Si or Si alloys)	25 800 1200 1350	99 ± 3 112 ± 3 157 ± 9 113 ± 5	4-point bend test; as-fabricated composite strength: 360 MPa at 25 °C
CVI-SiC/SiC composite system	ARCJoinT (carbonaceous mixture at the joint, cure, infiltrate with Si or Si alloys)	25 1200 1200	92 71 17.5[e]	Compression test on double-notched specimens, joints contain SiC + small amounts of Si and $TiSi_2$
SiC/SiC composite system	CA-glass ceramic (49.77% CaO + 50.23% Al_2O_3)	25	28	
SiC/SiC composite system	Co-10Ti braze, 1340 °C	25 25 700	51 in 7.5 min 55 in 15 min 75 in 15 min	
SiC/SiC composite system	Si-16Ti, Si-18Cr		71 ± 10 Ti, 80 ± 10 Cr	

a Ground.
b Unground.
c Combination of a ground and an unground specimen.
d Heat treated at 1000 °C.
e After 14.3 h in stress-rupture test at 1200 °C.

Figure 2.6: Representative values of shear strength of CMC joints.[3]

3 *Methodology*

3.1 Grid Core

At DLR, LSI process is selected to study the effect of different joining paste and joining methods for the manufacturing of C/C-SiC sandwich structure based on grid type core via in situ joining. In order to compare both folded and grid core geometry, the folded core parameters shown in Table 3.1 are used to determine the distance between the grids (w) [7]. The distance between the grids (w) was determined by using the following equations [7]:

Parameters	
Density (ρ)	1.9×10^3 kg/m^3
Thickness of the core (t_{core})	0.3 mm
Height of the core (h_{core})	13 mm
Core Weight	100 kg/m^3

Table 3.1: Folded Core Data [6]

Volume of the grid (V) = $[w^2 - (w-t)^2] * h = (w^2 - (w^2 - 2wt + t^2)) * h$

$$V = [2wt - t^2] * h \tag{3.1}$$

By using equation 3.1 ,
Mass of the grid (m) = (Volume of the grid)*ρ

$$m = [2wt - t^2] * h * \rho \tag{3.2}$$

$$V_{\text{total}} = w^2 * h \tag{3.3}$$

Substituting equation 3.2 and 3.3,

$$m/V_{\text{total}} = ((2wt - t^2) * \rho)/w^2 = 100 \;\; kg/m^3$$

$$100w^2 - 1.194w + (1.791 * 10) = 0 \tag{3.4}$$

Therefore, by solving equation 3.4, w = 12mm

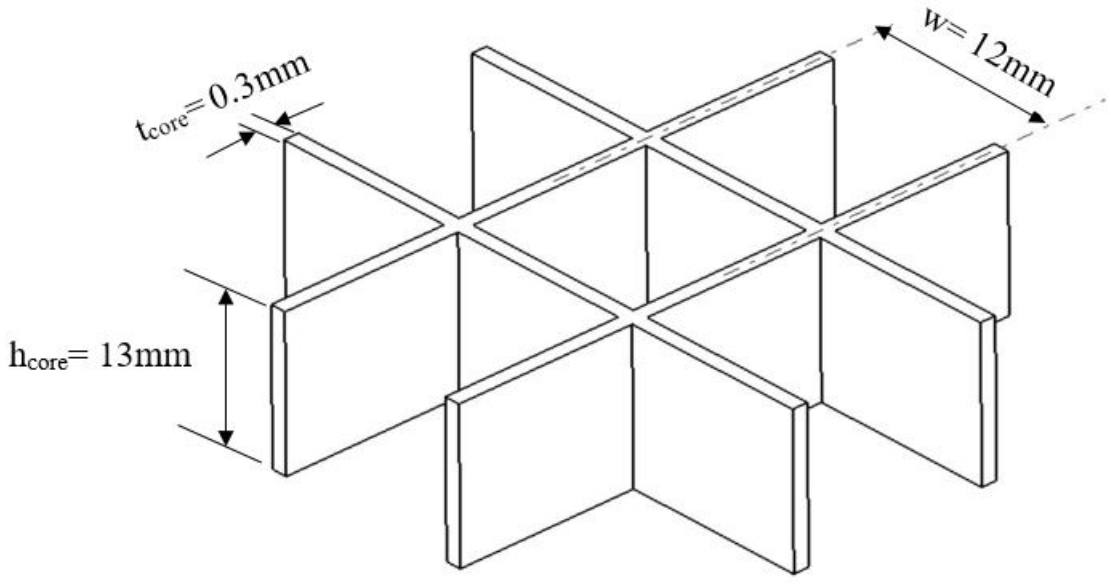

Figure 3.1: Dimensions of the Grid Core

The grid core is manufactured by interlocking the slotted uni-directional strips of C/C. The bi-directional grid as shown in Figure 3.1 offers advantages like high longitudinal stiffness, high strength per unit mass and ease of manufacturing [11] [12] [13]. The slotted C/C strips are manufactured by laser beam cutting technique. DLR outsources the machining of C/C slotted strips which makes the process time consuming. Thus, sample geometry which resemble the actual grid core sandwich structure is selected for tensile test analysis.

3.2 Tensile Test Sample

3.2.1 Sample Geometry

The three principles which were considered for selecting the tensile test sample geometry are [7]:

1. Maximum Mean Tensile Strength of the coupons.
2. Minimum Standard Deviation.
3. Uniform distribution of the force on the coupons while testing.

The first principle assists in determining the strength of the joining paste, the second principle helps in predicting homogeneity of the joint throughout the sample plate and the third principle assists in achieving reliable results. The tensile sample geometry which was selected is shown in Figure 3.2.

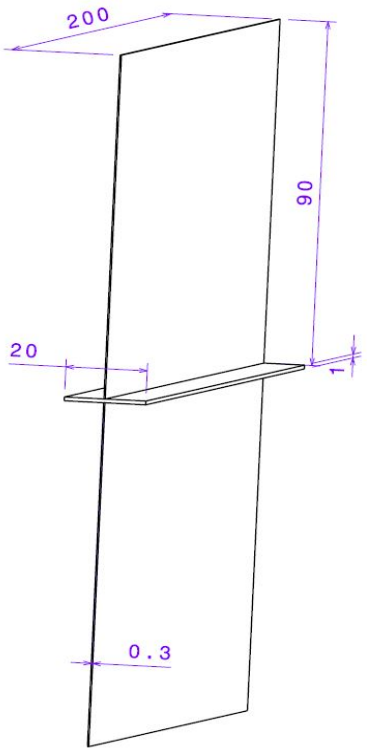

- No. of Components:1 Skin and 2 Cores
- Skin Dimension:$200mm \times 20mm \times 1mm$
- Core Dimension:$200mm \times 90mm \times 0.3mm$

Figure 3.2: Sample Plate Geometry for Tensile Test

3.2.2 Joining Paste

The joining paste is used for bonding the skin and core component of the tensile sample at C/C stage. The tensile samples were manufactured using both phenolic as well as epoxy joining paste[7].

Table 3.2 provides a ratio of resin to the additive with respect to the mass. JK60 and MGS LR285 are phenolic and epoxy resins respectively. PC40 is the carbon powder which is used as an additive to generate the SiC yield after siliconisation. The Ceramics department at DLR has been working with phenolic joining paste since past 15 years. Hence, it is considered as a reference joining paste. The

Resin	JK60	MGS LR285+ MGS LH285
Additive	PC40	PC40
Mixing ratio (Resin:Additive)	100:76	100:72

Table 3.2: Types of Joining Paste and Mixing Ratio

ratio of the epoxy joining paste was selected such that it matches the viscosity of the phenolic joining paste (18 Pa.s.). The hardener used for the curing of epoxy resin was MGS LH285 and the ratio of resin to the hardener was 100:40.

3.2.3 Manufacturing Procedure

The manufacturing procedure of the tensile samples is adapted from the research carried on C/C-SiC fold core sandwich structure. A schematic representation of the manufacturing procedure is shown below:

1. The core is held between two carbon plates as shown in figure 3.3 which are fixed with help of clamps.

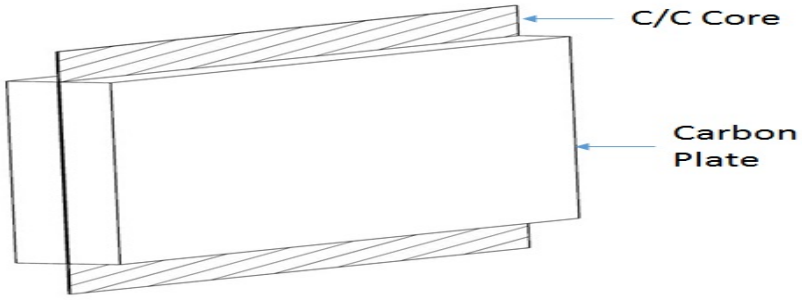

Figure 3.3: Core Setup

2. The steel blocks 1,2 and 3 were arranged on a steel plate as shown in figure 3.4. Clamp block 1 to the steel plate. The hatched portion is where the skin component is kept.

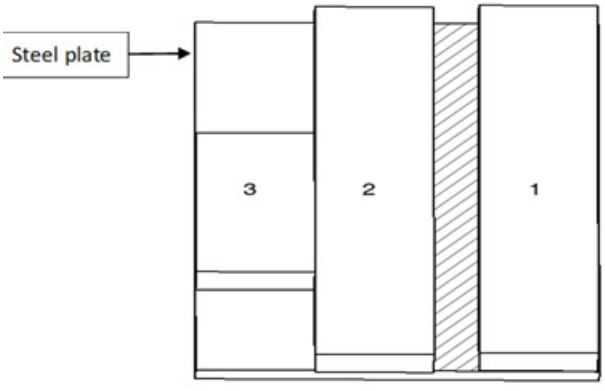

Figure 3.4: Arrangement of steel blocks and skin

3. Insert the core setup between the blocks in the hatched portion as shown in figure 3.5. Since the block 2 and 3 are not fixed, they can be adjusted so that the carbon blocks are firmly held between the blocks.

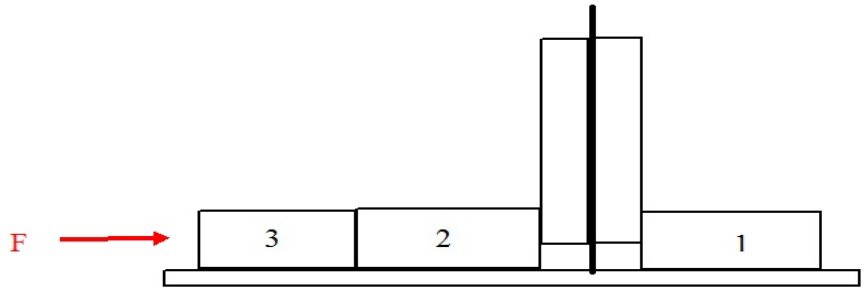

Figure 3.5: Adjustment of the blocks

4. Slightly clamp the block 3 so that it stays in the adjusted position. The reason for not clamping block 3 tightly is that later when the core setup is inserted, small tolerances can be adjusted.

5. Keep the Steel plate setup along with the skin component in the oven so that it is convenient to place the core setup after it is dipped in the joining paste. Core length should exactly match the skin length as the sample needs to be at the same level for the siliconsation process. This can be done by adjusting the skin component at the edge of the steel plate before joining.

6. On another steel plate, clamp a strip of 3mm thickness on the parallel edges of the plate as shown in figure 3.6. The joining paste thickness was selected based on the previous research performed on folded core C/C-SiC sandwich structures.

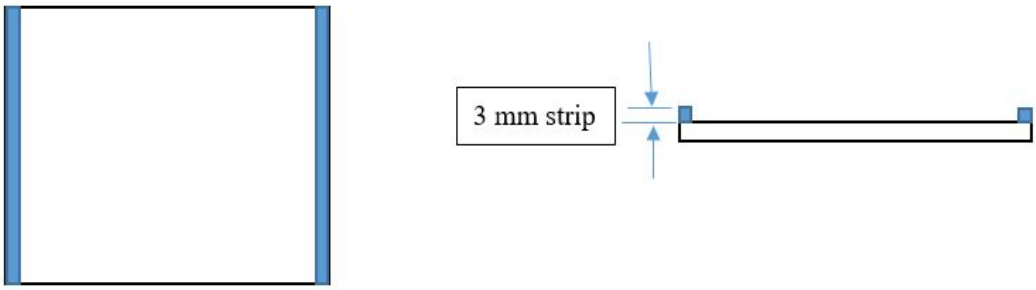

Figure 3.6: Joining paste thickness

7. Spread the paste in between the strip. Now to achieve an uniform height for the joining paste, use a plate and drag it with the support of the strip. For better uniformity, move the plate sideways while dragging.

Figure 3.7: Uniform distribution of the joining paste

8. Dip one edge of the core in the joining paste (with the core setup)as shown in figure 3.8.

   Note: While dipping the edge of the core the setup should be exactly perpendicular to the surface of the paste.

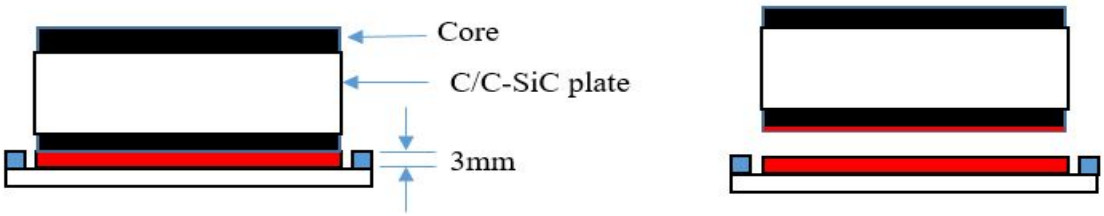

Figure 3.8: Dipping of core in the joining paste

9. The core setup is inserted between the block 1 and 2 as shown in figure 3.9 and a small force is applied on block 3 for adjusting the small tolerances so that the carbon plates are firmly held between block 2 and 1. Then depending on the type of joining paste used, the setup is either kept in the oven or at room temperature for curing. The cycle followed for the curing of phenolic joining paste is shown in figure 3.38.

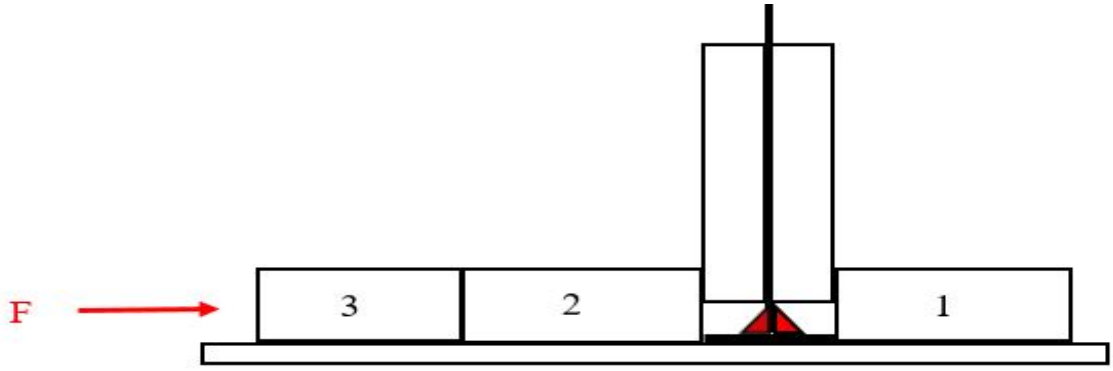

Figure 3.9: Final setup for first joint

10. The second joining takes place on the other side of the skin. The setup is aligned as shown in figure 3.10 so that both the cores are in line. If the cores are not in line then a moment will be generated while testing. The the steel block 1 is fixed with the steel plate using large clamps.

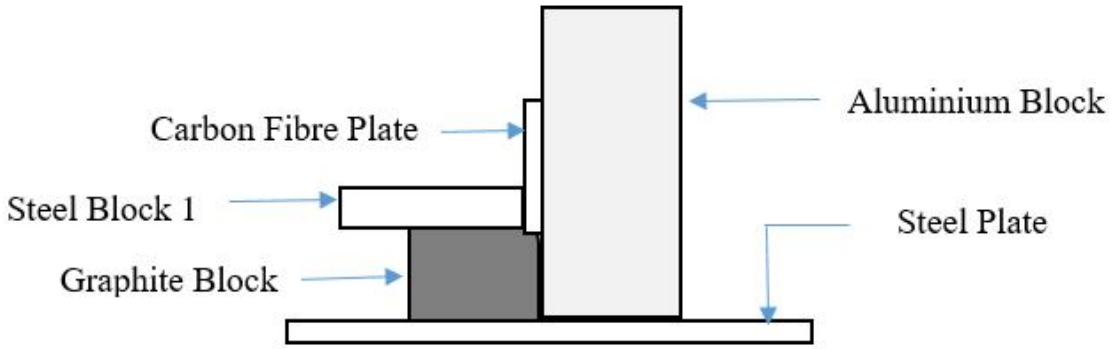

Figure 3.10: Setup alignment

11. The aluminium block and the carbon fibre plate is removed and a second graphite block and steel block 2 is placed. Then, the core setup is inserted besides steel block 1 and then steel block 2 as shown in figure 3.11. The block 2 is pushed with a little force in the direction of block 1 so that the core setup is held tightly.

    Note: The edges of the graphite blocks should be chamfered so that the radius of the first joint is not stressed.

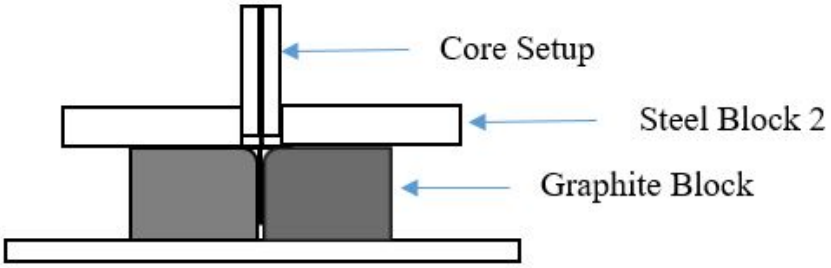

Figure 3.11: Final Setup for the second joint

12. Slightly Clamp the block 2 with the steel plate using large clamps so that later small tolerances can be adjusted and the carbon fibre plates can be firmly held between the steel blocks.
13. The dipping procedure of the core in joining paste is the same as step 6 to 8.
14. After dipping the core in the joining paste, insert the core setup between the steel blocks 1 and 2 and then adjust the small tolerances so that the carbon fiber plates are firmly held between the blocks. Now, clamp the block 2 tightly.
15. The curing process is similar to the one mentioned in step 9.

The siliconisation process will be explained elaborately in section 3.4

3.2.4 Results

3.2.4.1 Tensile Test

The formula used for determining tensile strength:

$$\sigma_{joint} = \frac{Force}{l_{joint} \times w_{joint}} \tag{3.5}$$

The tensile test results for phenolic and epoxy joining paste are shown in Table 3.3:

Joining Paste	Mean Tensile Strength of the Joint (MPa)	Standard Deviation
Phenolic	21	2.5
Epoxy	9.2	4.2

Table 3.3: Comparison between Phenolic and Epoxy Joining Paste [7]

3.2.4.2 Elemental Morphology

The SEM analysis of the tensile samples are shown in Figure 3.12a and 3.12b.Ideally there should be only three elements present in the joint. They are carbon, silicon and silicon carbide. The representation of different colours observed during SEM analysis is shown in Table 3.4.

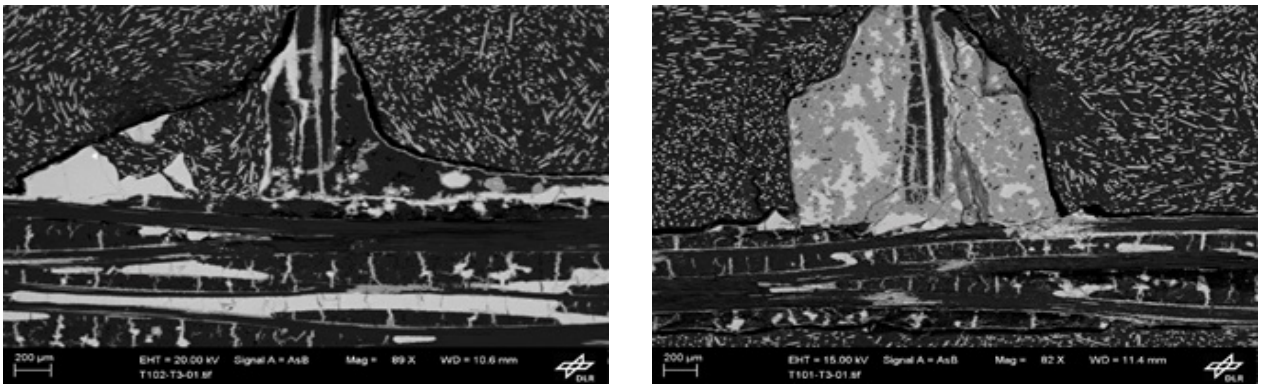

(a) Phenolic Joining Paste (b) Epoxy Joining Paste

Figure 3.12: SEM Analysis of the Joining Pastes [7]

Colour	Element
Dark Grey	Carbon
Grey	Silicon Carbide
White	Silicon

Table 3.4: Representation of Colours

From the SEM analysis of the tensile sample with phenolic joining paste, it was observed that lot of carbon was left in the joint after siliconisation, consequently making the joint unstable at high temperatures (carbon has the tendency to oxidise above 450^0C) [14]. The SEM analysis of the tensile sample with epoxy joining paste showed that almost all the carbon in the joining paste has been chemically converted to silicon carbide which makes the joint thermally stable as it avoids oxidation at high temperature [3] [15]. Although the sample with epoxy joining paste demonstrates high temperature resistance, the tensile strength of the joint is very low compared to the phenolic joining paste sample as seen in Table 3.3.

3.3 Shear Test Sample

In general, a sandwich structure often experiences two modes of stresses i.e. shear and bending and the joining paste which bonds the skin and core components of the structure is responsible for the transfer of the shear and normal stress from the skin to the core [5][16]. Therefore, shear test is chosen for the analysis of the joint.

3.3.1 Sample Geometry

The bi-directional grid core of the joined C/C-SiC sandwich structure is difficult to analyse because of multiple joining regions and the manufacturing of the slotted CFRP unidirectional strip is time consuming process as the strips have to be laser cut. Hence, a uni-directional web core geometry as shown in figure 3.13 was selected for the shear test. The factors which were considered for the selection of the sample geometry are:

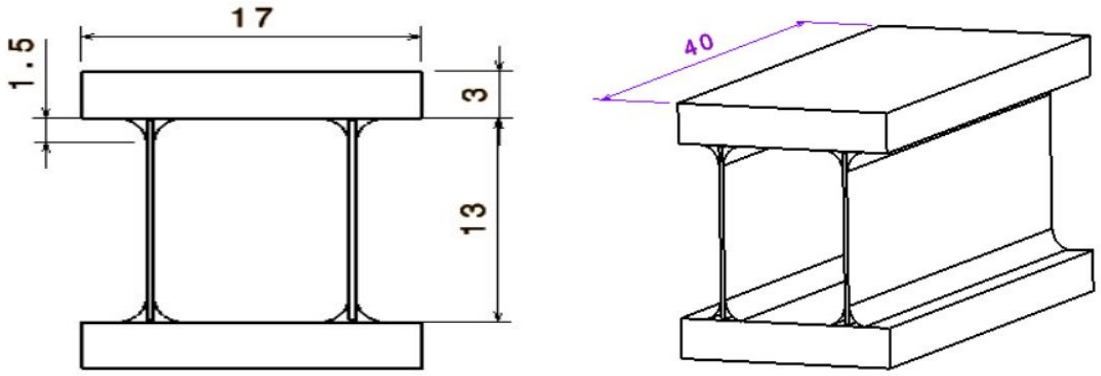

(a) Front View (b) Isotropic View

Figure 3.13: Shear Sample Geometry and Coupon Dimensions

1. Ease of Manufacturing – The C/C components are prepared with less sophisticated and inexpensive process like cutting and sawing.
2. Ease of Analysis - There are only two joining surfaces to be analysed.
3. Resemblance to the actual structure - The height and width is similar to the grid core based C/C-SiC sandwich structure.

The dimensions of the coupon were determined by carrying out shear test on coupons with different length and width, and observing the failure mode. Due to the lack of standardized test methodology, it becomes difficult to follow a particular dimension for the test [3].

3.3.2 Experimental Setup

The experimental setup for the shear test is selected based on the ASTM D7078/D7078M-05 standard. The test setup which was recommended initially is shown in figure 3.14.

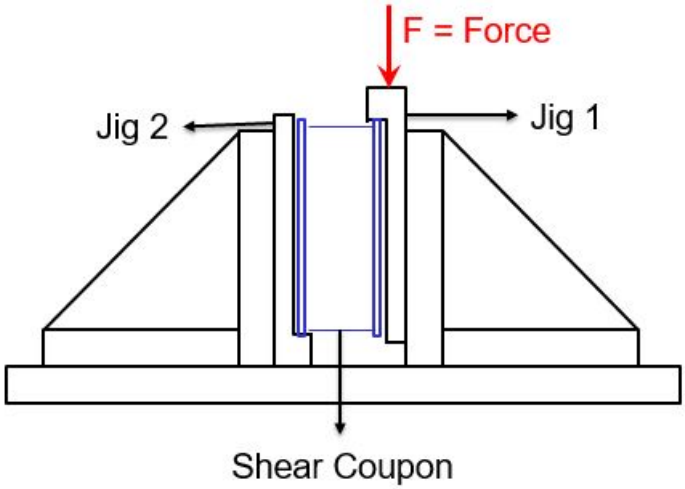

Figure 3.14: Type 1 Test Setup

In the Type 1 test setup, the shear coupon could be tested with two designs:

1. Coupon bonded to the Jigs.
2. Coupon not bonded to the Jigs.

A radius is machined on top of jig 1 where the force is applied so that the load is applied exactly at the middle of the jig. The coupon is also positioned in such a way that the applied force passes through the center of the coupon. Thus, avoiding non-uniform distribution of the force on the coupon.

A finite element analysis was performed on the test setup just to analyse and improve the test setup. Since the material properties of the manufactured shear coupon were unknown, a convergence study between the actual experiment and simulation could not be performed.

- The software used for performing the finite element analysis was ANSYS Workbench 17.
- The material properties used for the coupon are:

Property	**Unit**	**Skin Material**	**Core Material**
Young's Modulus in X direction	MPa	58000	34000
Young's Modulus in Y direction	MPa	58000	34000
Young's Modulus in Z direction	MPa	20000	11724
Poisson's Ratio XY		0.01	0.01
Poisson's Ratio YZ		0.1	0.1
Poisson's Ratio XZ		0.1	0.1
Shear Modulus XY	MPa	5140	3013
Shear Modulus YZ	MPa	6600	3869
Shear Modulus XZ	MPa	6600	3869

Table 3.5: Material Properties of the Skin and Core

- Ansys Composite Preppost (ACP) is used for the skin and core components and the joint is considered to be isometric with a poisson's ratio of 0.3 and shear stress of 11 MPa [8].
- The elements used for the coupon, joint and jigs are Solid 185, Solid 186 and Solid 186 respectively.

A general description of the simulated model is shown in figure 3.15.

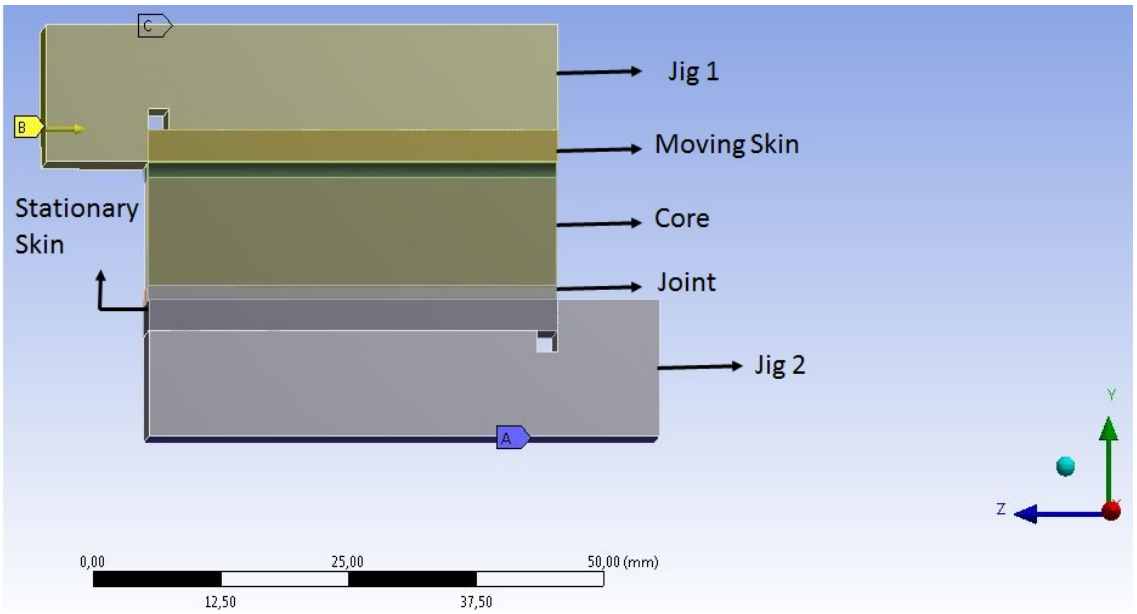

Figure 3.15: Boundary Conditions

A = Fixed Support
B = Displacement
C = Frictionless Support

Two boundary conditions were analysed:

1. 1^{st} boundary condition
   (a) Displacement of 0.7mm is applied on Jig 1 and frictionless support is applied on Jig 1.

(b) Jig 2 is fixed.

(c) Coupon is not bonded to the Jigs.

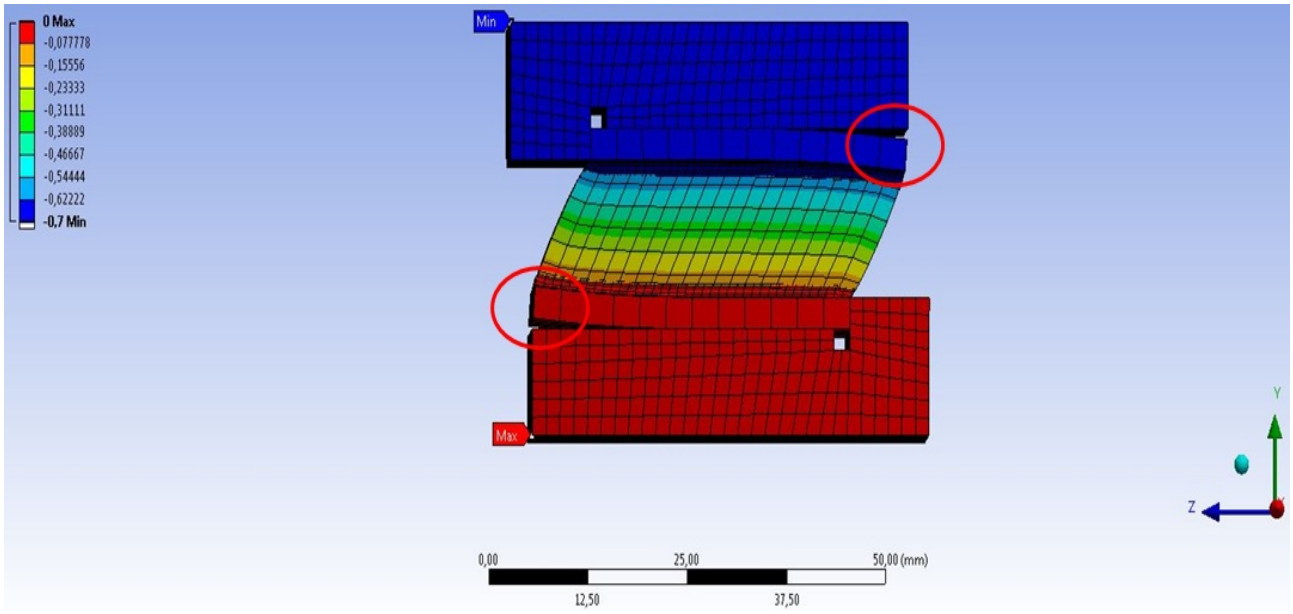

Figure 3.16: Deformation Analysis of 1st Boundary Condition

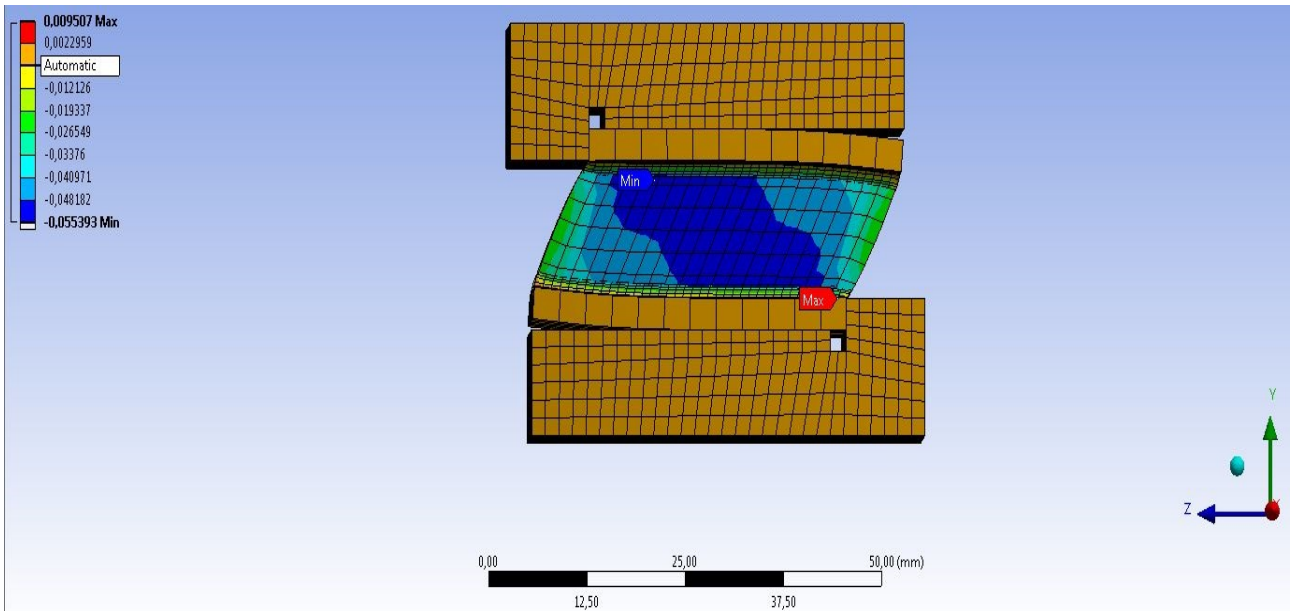

Figure 3.17: Shear Strain Analysis of 1st Boundary Condition

2. 2^{nd} boundary condition

(a) Displacement of 0.7mm is applied on Jig 1 and frictionless support is applied on Jig 1.

(b) Jig 2 is fixed.

(c) Coupon is bonded to the Jigs.

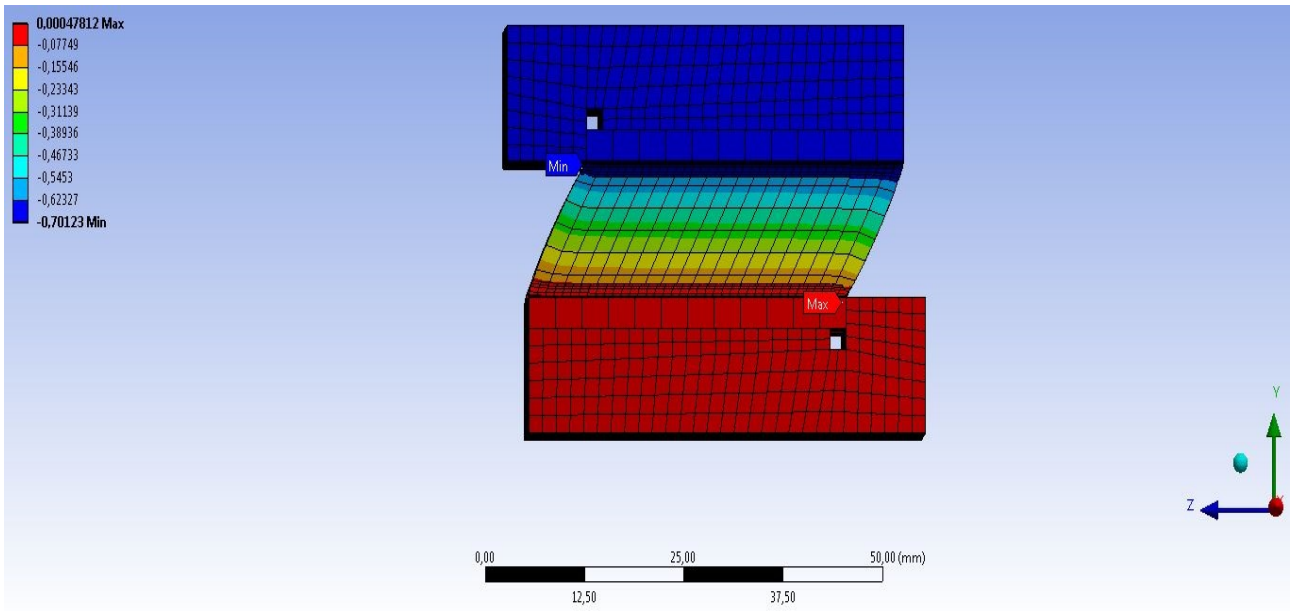

Figure 3.18: Deformation Analysis of 2nd Boundary Condition

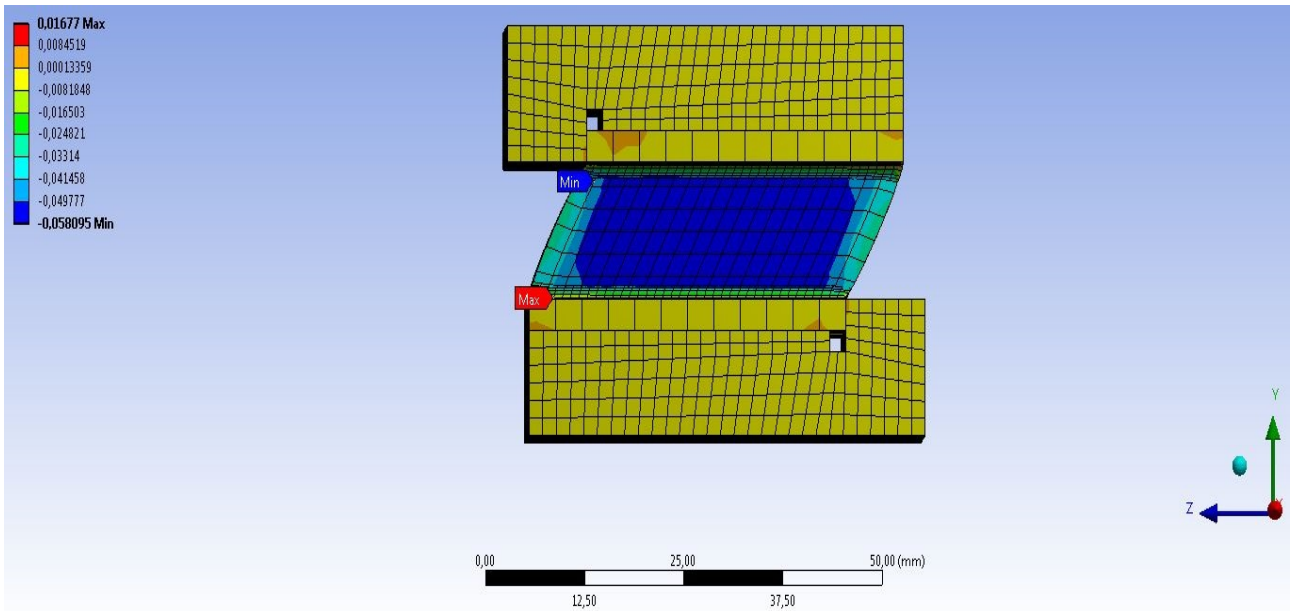

Figure 3.19: Shear Strain Analysis of 2nd Boundary Condition

The simulation was modelled with 3 layer C/C-SiC for core 20 layer C/C-SiC for the skin whereas the actual coupon was manufactured with 1 layer C/C-SiC for the core and 12 layer C/C-SiC for the skin.

It can be observed from figure 3.17 and 3.19 that the strain distribution is also refined by joining the coupon to the jigs. Even though the maximum strain value remains 5.8% but the uniform distribution of the strain assists in better Digital Image Correlation analysis. It can be also observed that when the coupon is not bonded to the jigs then the edges separate from the jigs as shown in figure 3.16 due to the Trellis effect

The major drawback was the time required to manufacture the pair of jigs shown in figure 3.14 (for 34 shear coupons) as the jigs had to be milled. Therefore, the geometry of the jigs was made less sophisticated as shown in figure 3.20.

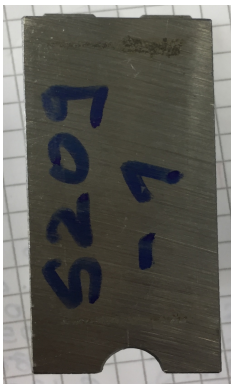

(a) Geometry of the new Jig

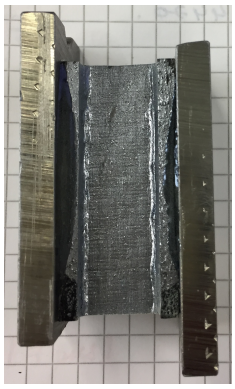

(b) Coupon bonded to the jigs

Figure 3.20: Shear Sample Geometry and Coupon Dimensions

The semi-circle has a diameter of 8.1mm and a roller pin of diameter 8mm will be used so that the load is transferred symmetrically through a point. The new test setup i.e. Type 2 test setup is shown in figure 3.21 where the rate of displacement was $1mm.min^{-1}$.

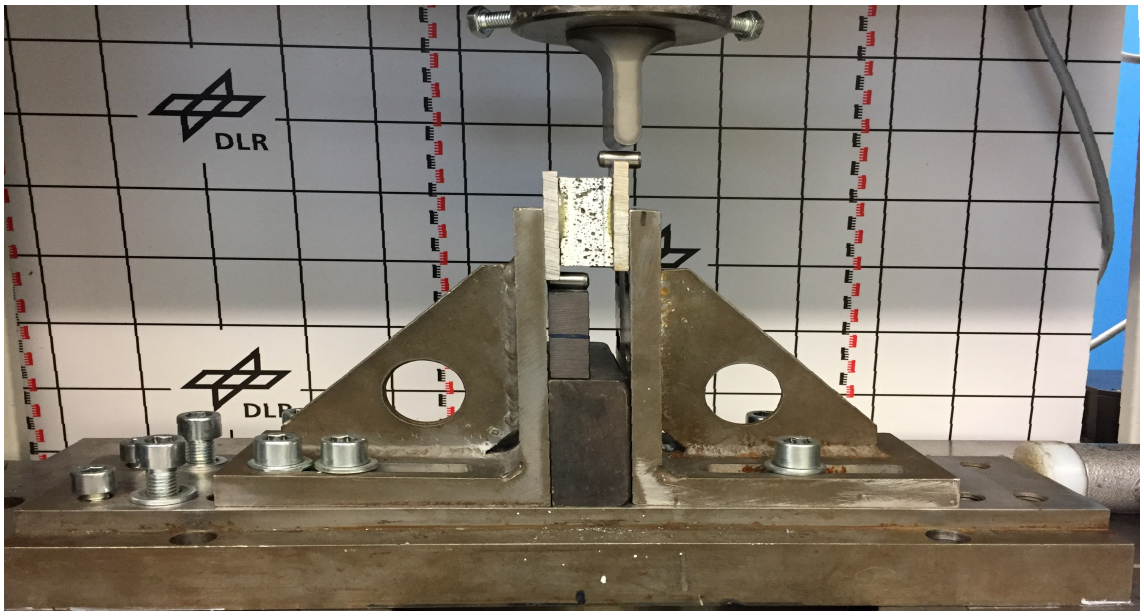

Figure 3.21: Type 2 Test Setup

The coupons are bonded using AW106 epoxy resin and HV953U hardener. The resin to hardener ratio is 100:80. The epoxy mixture is partially cured at room temperature for 1 hour and then the curing process is sped up by heating the whole setup at 70 degrees for 8 hours. After the test, the coupons are separated by heating the setup shown in figure 3.20b at 220 degrees for half hour. The procedure is repeated for next set of coupons. A high resolution camera is also focused on the sample which is used for the Digital Image Correlation. Digital Image Correlation is explained in section 3.3.3.

3.3.3 Digital Image Correlation (ARAMIS)

The strength of the joint will be determined through the shear test but the shear strain cannot be determined through conventional methods because:

1. The joining layer is about 2mm thick and has a meniscus which makes the application of strain gauge difficult.
2. The strain gauge cannot be fixed on the core as the thickness of the core is low (0.3mm). Hence, the glue which is used to fix the gauge stiffens the core.

Thus, Digital Image Correlation (ARAMIS software) is used for determining the shear strain.
In reality ideal shear test is difficult to achieve because of following reasons:

- Buckling
- Bending
- Settings of test machine.
- Stiffness of specimen holders.

But the test setup can improved to minimise the influence of the external factors. Procedure for calculating shear strain by using ARAMIS is as follows:

1. The sample needs to be prepared by coating the surface which is to be analysed with a white paint and then a random speckle pattern of black paint is sprayed on the white coating as shown in figure 3.22.

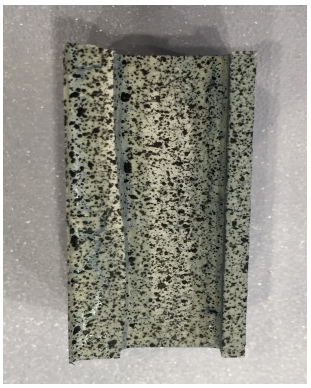

Figure 3.22: Sample Preparation for ARAMIS

2. For accurate analysis, the speckle pattern should be coarse and have a maximum diameter of 1mm (approx). **NOTE:** The diameter of the black speckle depends on the maximum strain experienced by the structure i.e. lower strains = smaller (finer) diameter.
3. In our case, a high resolution camera (14,3 Megapixel) with external lens (58mm) was fixed on a tripod and focused on the front view of the sample. The maximum resolution for the sandwich sample is 236 MP/mm. It should be noted that only the analysis area should be captured to get the highest local density of measuring points.
4. The images are taken after an interval of 5 seconds till the failure of the sample. All the images are imported to ARAMIS.
5. The algorithm parameters, i.e. facet size and distance have to be adapted for the evaluation of shear test. Facet is a square box which surrounds the stage point as shown in figure 3.24a. It is very important that there is a colour contrast within the facet as the software tracks this change in contrast for the interpolation of the images.

6. Adjusting facet size is similar to the meshing of a specimen during finite element analysis i.e. the facet size should not be too big or too small as both can affect the accuracy of the interpolation. The recommended facet size and distance for ASTM standards is 25x25 pixels and 15x15 pixels respectively.

7. An analysis area has to be selected for the shear analysis. It should be taken care that the analysis area is not larger than the coupon. In figure 3.23a, it can be seen that the interpolation changes with respect to the analysis area which affects the accuracy of the results. In our case, the difference between the displacement of the skins will be analysed. The analysis area as shown in figure 3.23b

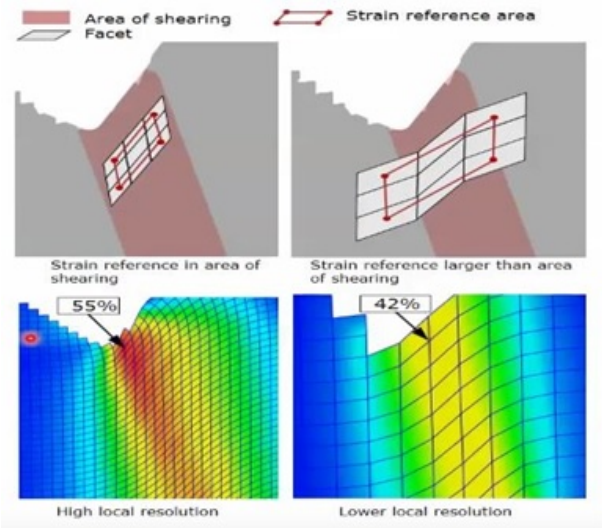

(a) Effect of Analysis Area

(b) Analysis Area for the Coupon

Figure 3.23: Analysis Area

8. After the selection of the analysis area, stage points are select within the analysis area i.e. assigning facets for a particular area which has colour contrast (white and black region). In figure 3.24a and 3.24b it can be observed that the facet shape changes from square to rhombus as the sample is deformed. The analysis area is interpolated based on this deformation.

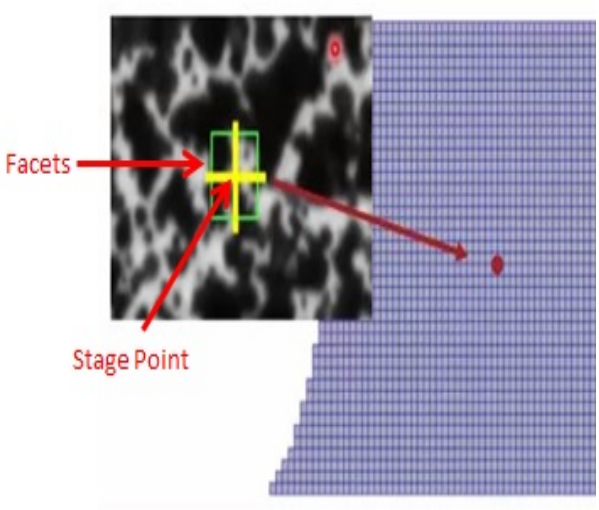

(a) Before Deformation

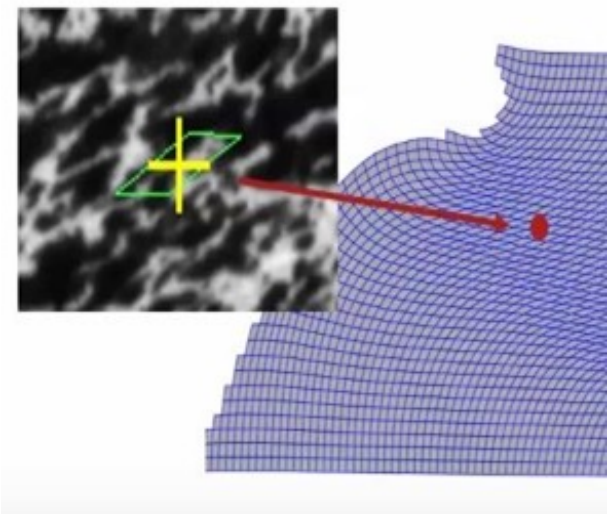

(b) After Deformation

Figure 3.24: Facet Deformation [17]

In our case, the facets position will be changed instead of the shape as the skins of the coupon

will only undergo vertical displacement. The figure 3.25 shows the facet and stage point selection for the coupon.

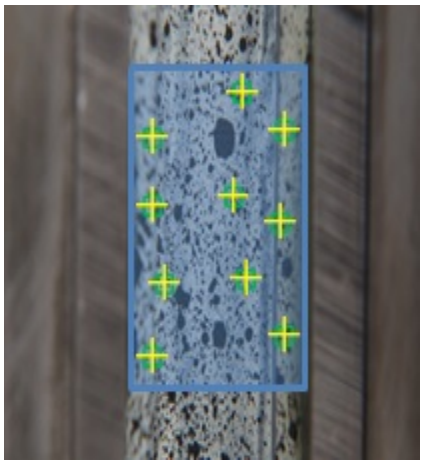

Figure 3.25: Face Selection for the Coupon

9. After interpolation, 3 displacement points are selected on the stationary surface and moving surface as shown in figure 3.26.

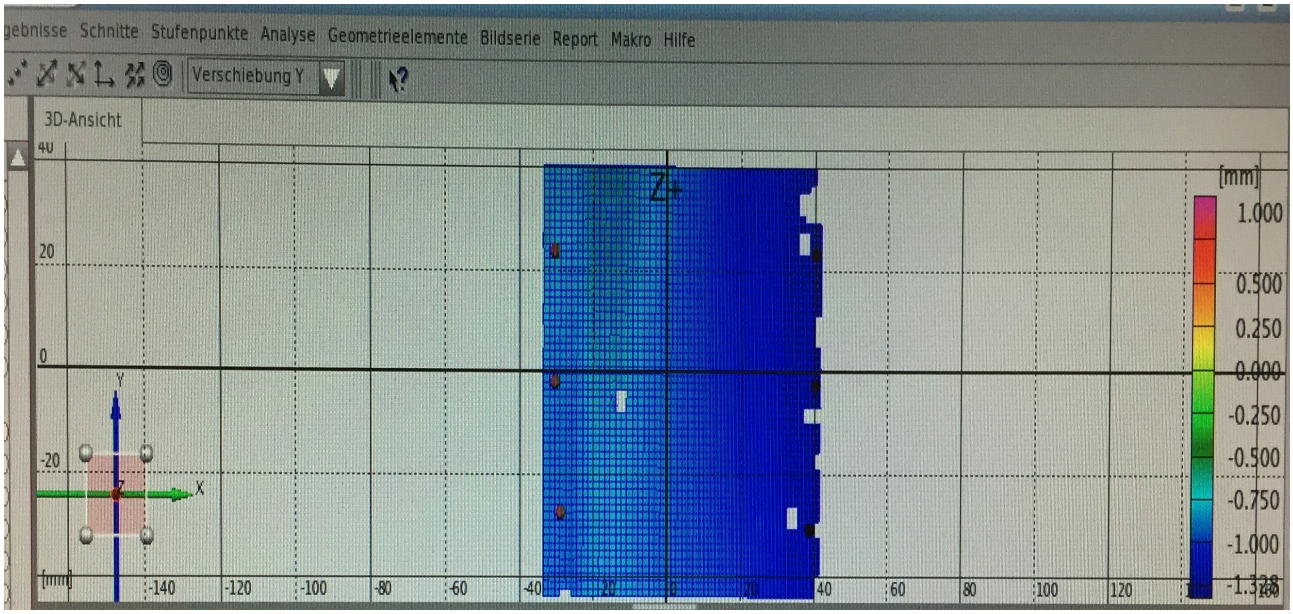

Figure 3.26: Interpolation of the analysis area and selection of displacement points (Left:Stationary Surface, Right:Moving Surface)

10. A force vs displacement graph is obtained based on the points selected on the stationary and moving surface as shown in figure 3.27.

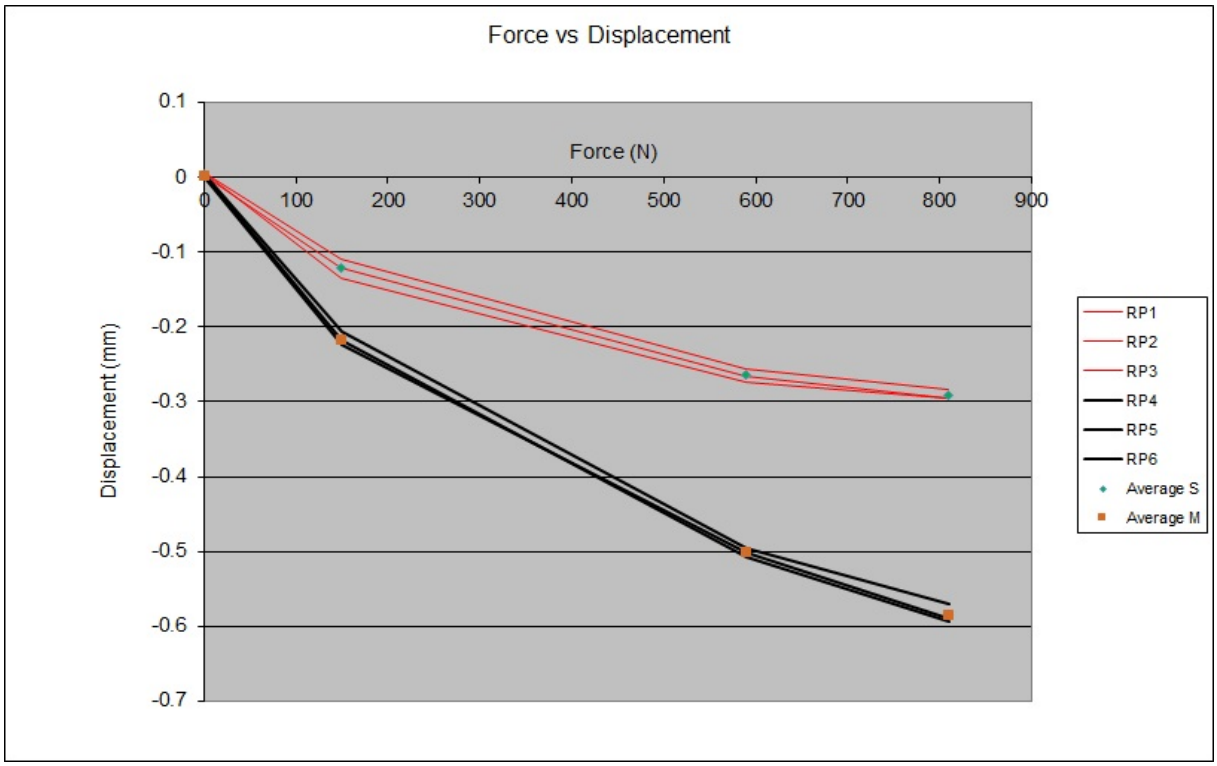

Figure 3.27: Force vs Displacment graph

11. The data from the graph is exported to Microsoft Excel. As shown in figure 3.27,
    Average S = average of the stationary surface at a each load interval
    Average M = average of the moving surface at each load interval

12. The shear strain is determined by:

$$tan\gamma \sim \gamma = \frac{\Delta x}{h_c} \tag{3.6}$$

γ = Shear Strain.
Δx = Average M - Average S.
h_c = Height of the core.

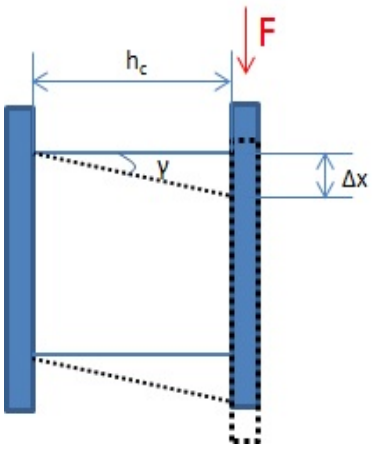

Figure 3.28: Shear Strain Principle for Shear Coupon

13. The load is noted down for each time interval i.e. for each pic that is taken during the test and shear stress is determined by using the following formula:

$$\tau = \frac{Load}{Area} = \frac{F}{n * l * t_w} \tag{3.7}$$

n = no. of Web(s)

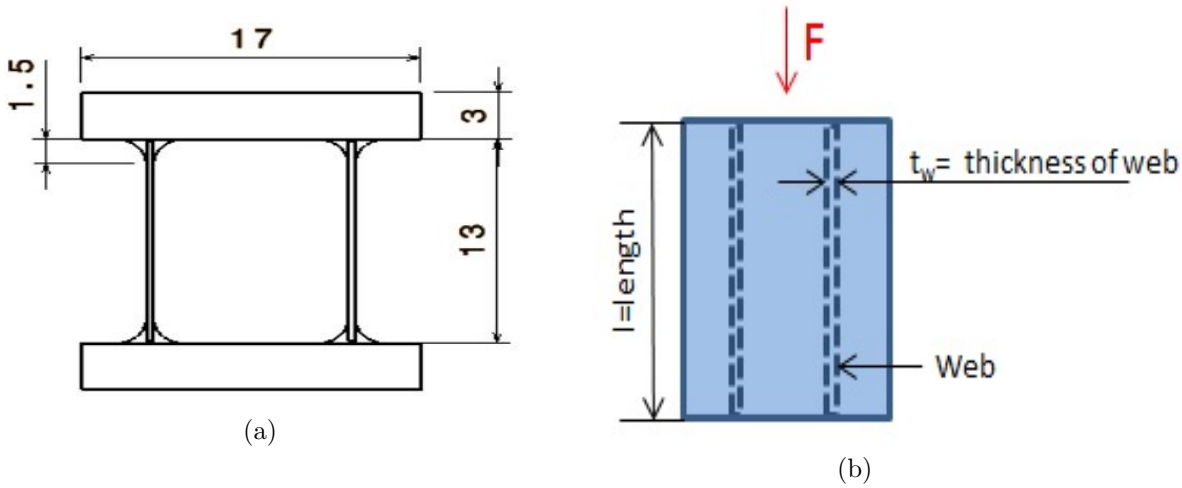

Figure 3.29: Front and Top View of the Shear Coupon

14. The shear modulus of the core is determined by:

$$G = \frac{\tau}{\gamma} = \text{slope}(\tau; \gamma) \tag{3.8}$$

The slope of the shear stress vs strain curve as shown in figure 3.30 gives the shear modulus of the structure.

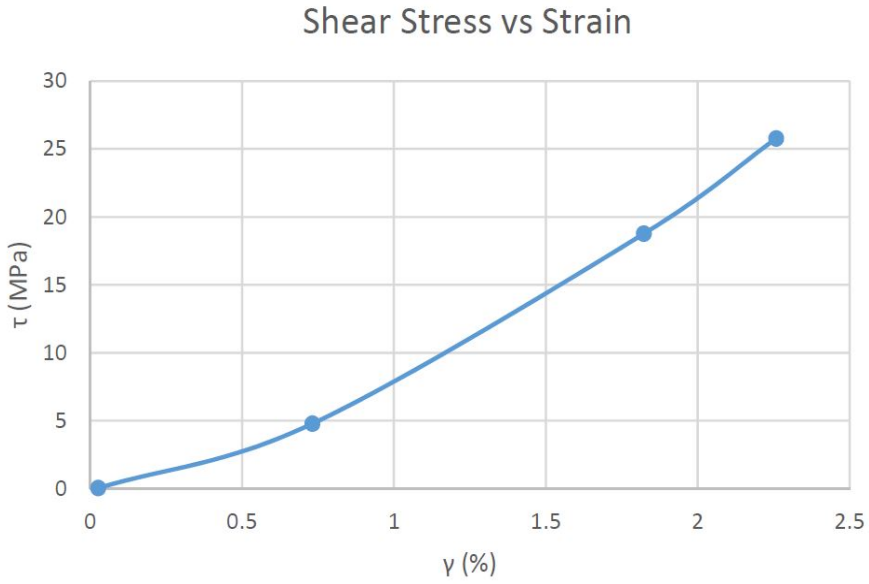

Figure 3.30: Shear Stress vs Strain Curve

3.3.4 SEM Analysis

The SEM analysis is used to determine the elemental configuration of the joint. The dimensions of the sample required for the SEM analysis are 15x15x5. The length and width of the sample should not exceed 15mm whereas the thickness should not be less than 5mm.

The sample can be embedded either by using KonductoMet powder in an embedding machine or by infiltrating a mold with epoxy resin under vacuum. The sample is embedded in 5 mins in the machine whereas it takes 12 hours for the epoxy resin to be cured. An EpoFix resin and hardener in the ratio of 25:3 are used for embedding the sample.

Even though the machine takes shorter time, it cannot be used for the shear coupons because a high pressure is exerted on the sample which might break the thin webs (0.3mm) as shown in figure 3.31a.

(a) Machine Embedded Sample (b) Epoxy Embedded Sample

Figure 3.31: Top View of the Coupon

The samples are polished by using a polishing machine. After polishing, the samples are kept in an ultrasonic bath inside a beaker containing osmosis water for 15-20 mins. The ultrasound bath assists in cleaning the surface of the sample. After the ultrasound bath,the samples are kept in the oven for drying.

Since the epoxy resin is non conductive, it is coated with platinum so that the surface captures the electrons for better analysis. Along with SEM, Energy Dispersive X-ray is used to distinguish between the elements based on the different colours captured in SEM but EDX cannot be used for quantifying the elements because it is not accurate for lower atomic number elements such as carbon, boron, nitrogen, oxygen, etc. Therefore, histogram technique is used in CorelDRAW to quantify the mass percentage of individual element present in the joint.

3.3.5 Manufacturing Process for Shear Sample Plate

3.3.5.1 Joining of Carbon/Carbon Components

The joining procedure for the shear sample plate is as follows:

1. The webs are held between three C/C-SiC beams which are fixed with help of screws and bolts as shown in figure 3.9.

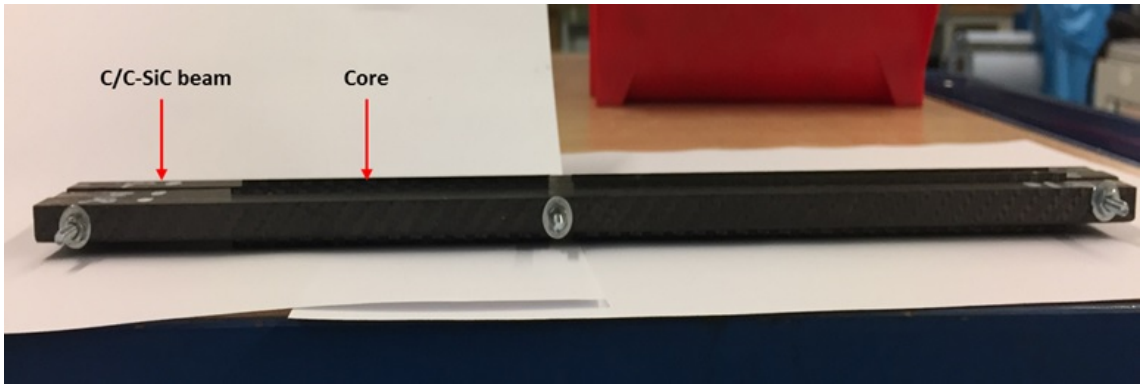

Figure 3.32: Core Setup

2. The steel blocks 1,2 and 3 were arranged on a steel plate as shown in figure 3.33. Clamp block 1 to the steel plate. The hatched portion is where the C/C skin component is kept.

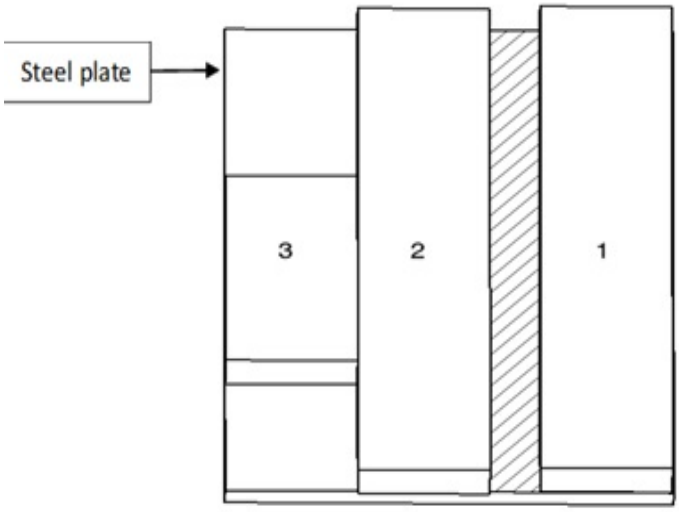

Figure 3.33: Arrangement of the steel blocks and skin plate

3. Insert the core setup between the blocks in the hatched portion as shown in figure 3.34. Since the block 2 and 3 are not fixed, they can be adjusted so that the core setup is firmly held between the blocks. Care should be taken that the joining is symmetric.

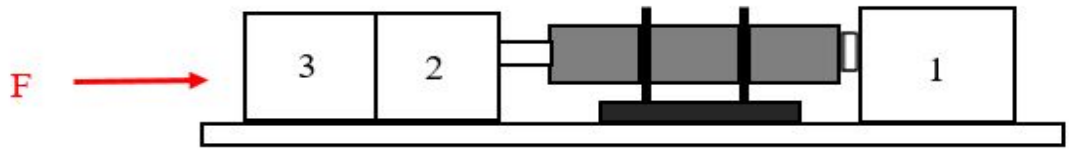

Figure 3.34: Adjustment of the blocks

4. Slightly clamp the block 3 so that it stays in the adjusted position. The reason for not clamping block 3 tightly is that later when the core setup is inserted with the joining paste then small tolerances can be adjusted.

5. A wooden block is grooved with a depth of 3mm. The groove is filled with the joining paste and a triangular spatula is used for the uniform distribution of the paste throughout the groove as shown in figure 3.35a and 3.35b. Thus, a homogeneous distribution of the joining layer is achieved on the core.

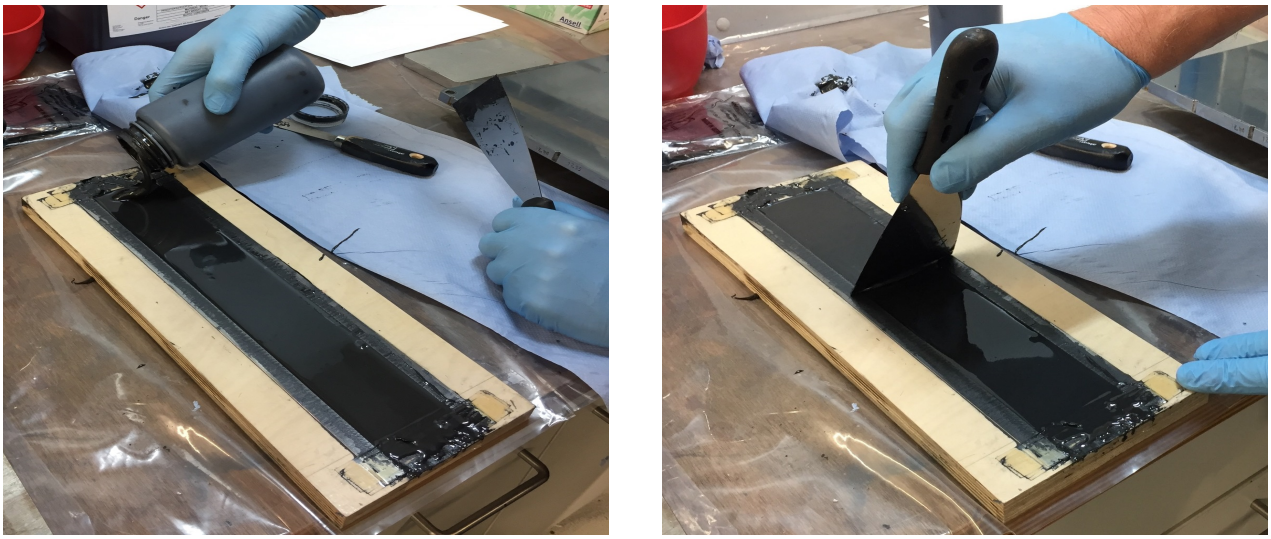

(a) (b)

Figure 3.35: Uniform Distribution of the Joining Paste

6. The core setup is vertically dipped in the joining paste, assisted by the guiding block as shown in figure 3.36.

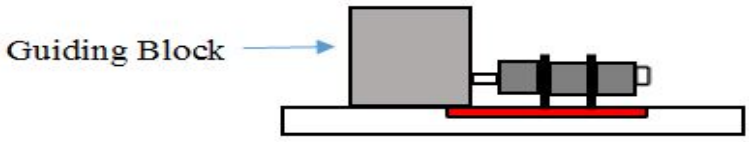

Figure 3.36: Core dipped in the Joining Paste (Red)

7. Step 3 is followed again and the block 3 is clamped tightly. Pressure is applied on the core setup by keeping metal blocks on top of it so that the core touches the skin as shown in figure 3.37.

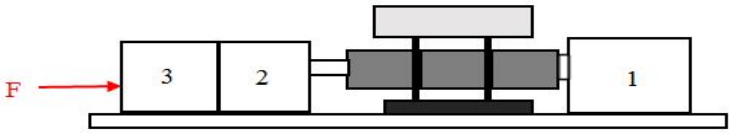

Figure 3.37: Pressure block on the Core Setup

8. If phenolic joining paste is used then the whole setup is kept in the oven at pre-programmed curing cycle as shown in figure 3.38 whereas epoxy joining paste is cured at room temperature but the curing time depends upon the joining paste configuration.

9. The same procedure is followed for joining the other side of the sample plate.

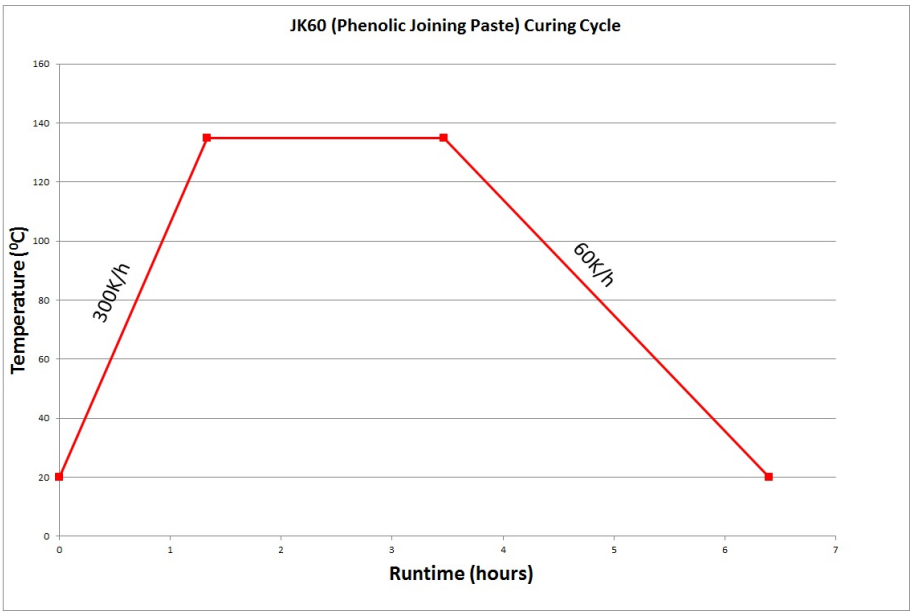

Figure 3.38: Curing Cycle for Phenolic Joining Paste

The manufacturing technique was improved by:

1. Degassing the resin so that the air bubbles inside the joining paste are reduced.
2. A grooved wooden block of defined depth of 3mm was used so that the thickness of the joining paste layer on the core is uniform.
3. Instead of infiltrating silicon with respect to the total mass of the structure, different percentage of silicon is infiltrated for the core and the skin which assists in avoiding excess silicon infiltration in the structure.

3.4 Siliconisation

After the sample plates are cured, they are kept for siliconisation by using LSI technique. The Si crystals are spread around the structure in a specific proportion. The proportion of Si infiltrated is given by Equation 3.9 and 3.10: For 0.3mm thick Core component,

$$m_{\text{Si-Core}} = 200\% \times m_{\text{C/C-Core}} \tag{3.9}$$

For any component greater than 0.3mm thickness,

$$m_{\text{Si-Skin}} = 45\% \times m_{\text{C/C-Skin}} \tag{3.10}$$

where,
m_{Si}= mass of the silicon infiltrated.
$m_{C/C}$= mass of the sample plate before siliconisation.

The sample is kept on a Boron Nitride (BN) coated plate and the Si crystals are spread around the sample. The Si crystals melt inside the siliconisation furnace and infiltrates in the structure because of the capillary action of the porous C/C material [3]. During siliconisation, the joining paste is pyrolysed to porous carbon and subsequently infiltrated with molten Si and gets chemically transformed into SiC which makes the joint thermally stable by avoiding oxidation at high temperature [3]. After siliconisation, the sample plate is cut into coupons of the dimension 40x19x17mm for testing. A sawing machine with a diamond coated sawing blade was used for cutting the sample plate into coupons.

4 *Variations of Joining Paste*

The main goal of the thesis is to develop a joint which contains more than 50% SiC and has a shear strength above 11 MPa. Thus, to achieve this goal different configuration joining pastes were tested. The variation of the joining pastes were decided based on the previous research as mentioned in chapter 3.2. The resin and additive used for the different types of joining paste are:

1. JK60 Phenolic Resin.
2. L285 Epoxy Resin and MGS LH285 Hardener.
3. PC40 Carbon Powder.

Sample No.	**S203**	**S204**	**S205**	**S206**	**S207**	**S208**	**S209**	**S210**
JK60 Resin	✓	✓	✓	✓	-	-	✓	✓
L285 + MGS LH285 Resin	-	-	-	-	✓	✓	✓	-
Additive	PC40	PC40	PC40	PC40	PC40	PC40 + 6g Acetone	PC40	PC40
Mixing Ratio (Resin or Resin + Hardener : Additive)	100:76	100:68	100:60	100:76	100:72	100:108	100:60:120	100:76
Comments	0.7mm thick core	10% less PC40 w.r.t. S206	20% less PC40 w.r.t. S206	Reference Phenolic joining paste	Epoxy joining paste	50% more PC40 w.r.t. S207	Phenolic epoxy joining paste combination	Gap of 0.15mm

Table 4.1: Variation of Joining Pastes.

- In section 3.2.2, it is stated that the phenolic joining paste is considered as a reference joining paste. Therefore, a reference sample plate S206 is manufactured with the phenolic joining paste configuration for shear analysis.
- The proportion of PC40 in sample plate S204 and S205 is reduced by 10% and 20% respectively compared to reference joining paste because from the previous research it was observed that more than 50% residual carbon was left in the joint after siliconisation. The presence of excess carbon reduces the stability of the joint at high temperature as carbon oxidises around 700^0C.
- The epoxy joining paste cures at room temperature and does not contain a lot of carbon residual but the tensile strength is low compared to the reference phenolic joining paste. To test the shear properties of the epoxy joining paste which was used in section 3.2.2, sample plate S207 is manufactured.
- An increase in the residual carbon content is the key to add strength to the epoxy joining paste. Hence, sample plate S208 was manufactured with 50% more PC40 content than S207 and 6 grams of acetone was added to retain the viscosity mentioned in section 3.2.2.
- An innovative combination of epoxy and phenolic resin along with the addition of PC40 was researched so that the room temperature curing is achieved and the strength of the joining paste is also not compromised. The optimum configuration for the phenolic epoxy joining paste is selected based on the fulfillment of all the reasons mentioned below:
  1. Fastest room temperature curing time.
  2. Lowest epoxy content.

3. Carbon content before and after pyrolysis should be close to the reference phenolic joining paste but not lower than epoxy joining paste. Therefore, the optimum configuration can be compared to the reference phenolic joining paste.

	A	**B**
Resin and Resin + Hardener : Additive	**JK60 : PC40**	**L285 + MGS LH285 : PC40**
Mixing Ratio	**100 : 76**	**100:72**
Total quantity (g)	**176g**	**172g**

Table 4.2: Ratio and Quantity of Reference Phenolic Joining Paste (A) and Epoxy Joining Paste (B)

Table 4.2 represents the ratio and quantity of reference phenolic joining paste and epoxy joining paste respectively. In the experiments conducted by mixing phenolic and epoxy joining paste as shown in table 4.3, the ratio and quantity of reference phenolic joining paste i.e. Anew was kept constant whereas in epoxy joining paste, i.e. Bnew only the ratio of epoxy joining paste was kept constant but the quantity was varied. PC40 (Anew + Bnew) is the carbon yield before pyrolysis as the carbon yield before the pyrolysis is from PC40 carbon powder.

Experiment No.	**Anew (g)**	**Bnew (g)**	**Curing time (h)**	**PC40 (Anew + Bnew) (%)**
1	176	17	60	43.1
2	176	34	60	43
3	176	52	48	42.9
4	176	69	48	42.8
5	176	86	36	42.7
6	176	94	6	42.7
7	176	120	6	42.6

Table 4.3: Combinations of Phenolic Epoxy Joining Paste (Before Pyrolysis)

After pyrolysis, the residual carbon yield from the epoxy resin is 20-30% of the resin mass-% and for phenolic resin it is 55-70% of the resin mass-% [18]. Therefore,

$RC_{\text{epoxy}} = 20\% \times$ mass of epoxy resin

$RC_{\text{phenolic}} = 55\% \times$ mass of phenolic resin

$RC_{\text{total}} = RC_{\text{epoxy}} + RC_{\text{phenolic}} + \text{PC40}$

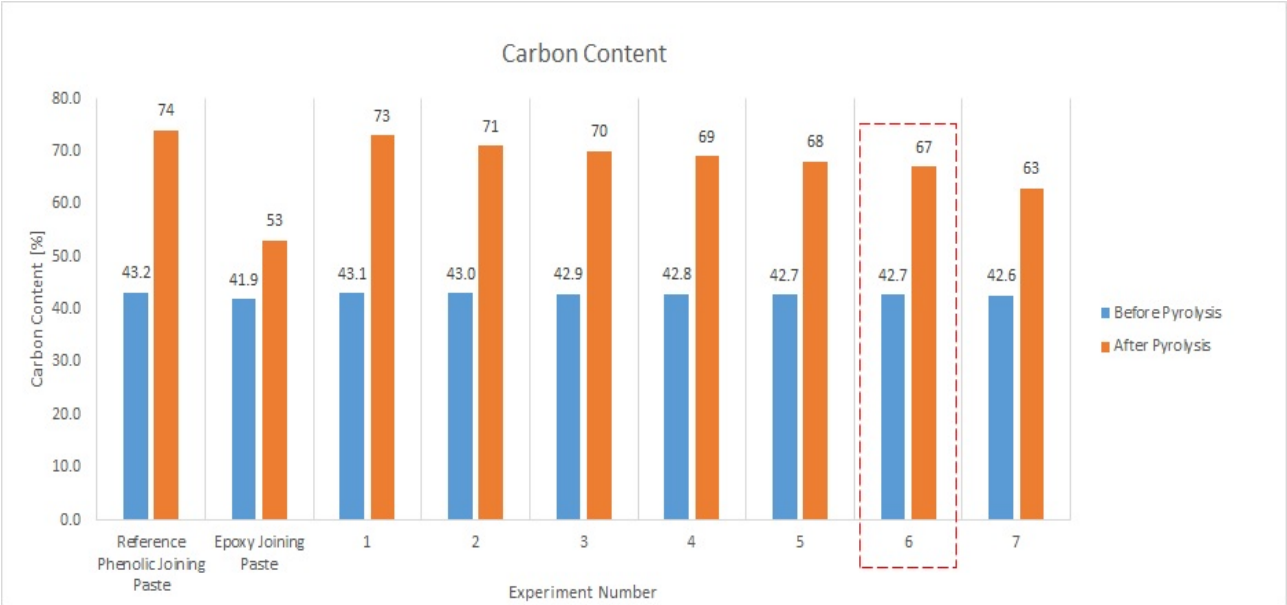

Figure 4.1: Carbon Content Before and After Pyrolysis

The experiment number '6' satisfies all the criteria required for the optimum configuration of the phenolic epoxy joining paste i.e.

1. The exp.no.6 joining paste cures at room temperature in 6 hours which is faster than all the previous combinations.
2. It has the lowest epoxy content compared to experiment no. 7 which also cures in 6 hours.
3. The carbon content before pyrolysis is 42.7% and after pyrolysis is 67% which is close to the reference phenolic joining paste and more than epoxy joining paste as shown in figure 4.1.

In other words, the optimum configuration for JK60 : L285 : PC40 is 100:60:120.

4.1 Gap Analysis

The major reason for the generation of gap between the skin and core as shown in figure 4.2 is manufacturing tolerances.

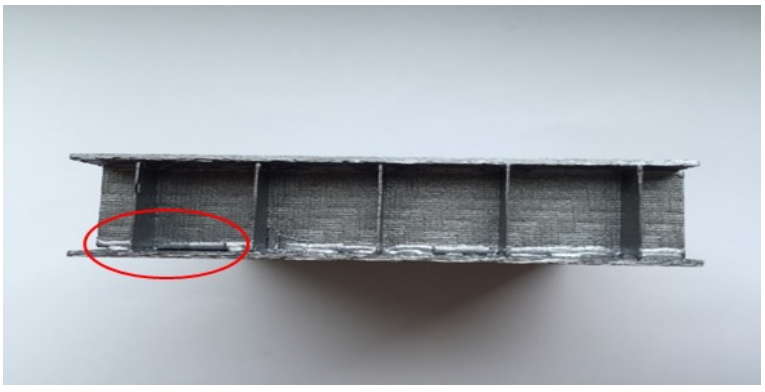

Figure 4.2: Gap generated due to manufacturing tolerance

In order to assure that the core components are cut according to the exact dimensions, sophisticated techniques like laser cutting and water jet cutting are used which increase the machining cost. Hence, the gap between the skin and core is analysed to ensure that the structure can withstand the shear load close to the reference phenolic joining paste. If the structure successfully withstands the shear load close to the reference phenolic joining paste then less sophisticated techniques with more tolerances like

cutting and sawing can be used for the machining of the webs which will in turn reduce the machining cost. Thus, it is important to analyse the allowable gap and the effect of the gap on the shear strength of the coupon.

To determine the allowable gap, a wedge sample was manufactured as shown in figure 4.3.

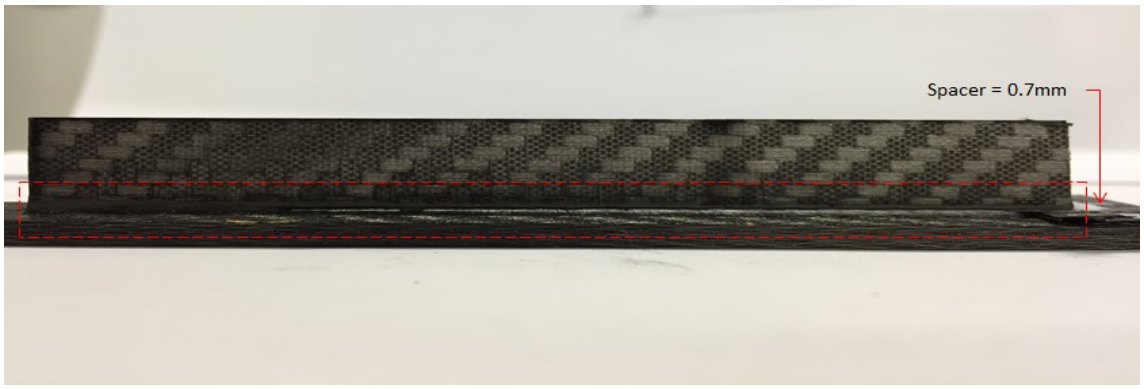

Figure 4.3: Wedge Sample

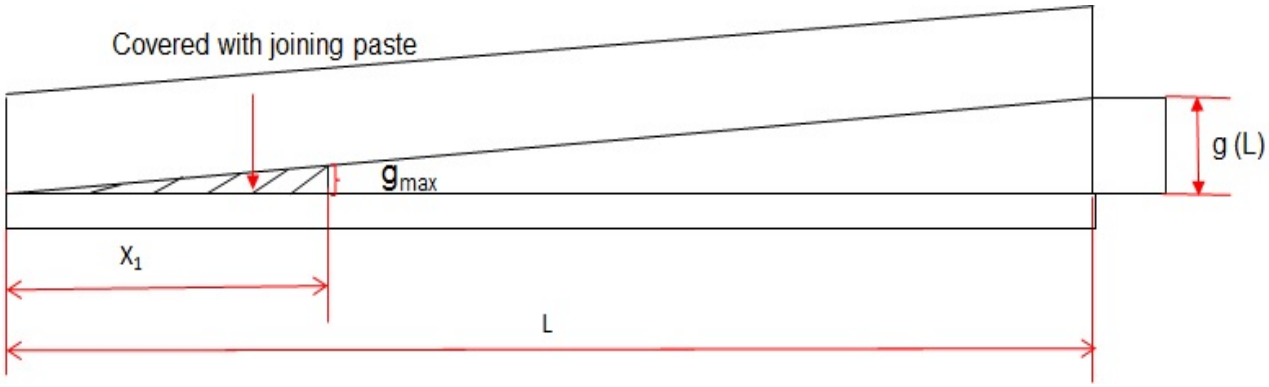

Figure 4.4: Schematic Representation of Wedge Sample (area marked in red).

Therefore, by using the concept of similar triangles:

$$g_{max} = g(L) \times \frac{X_1}{L} \tag{4.1}$$

$$g_{max} = 0.7 \times \frac{23}{89} \tag{4.2}$$

$g_{max} = 0.18mm$

The reference phenolic joining paste was used to manufacture sample plate S210 with a constant gap of 0.15mm between the skins and core. The constant gap was maintained by using spacer of 0.15mm at both the ends of the sample plate. The shear strength of the S210 coupons (with gap) will be compared to reference phenolic joining paste S206 coupons (without gap).

5 *Results and Discussion*

5.1 ARAMIS Reproducibility and Reliability

First Experiment: The C/C-SiC sandwich structure undergoes very small displacement (approx. 1mm max.). Therefore, the reliability and reproducibility of ARAMIS had to be tested. Three experiments were carried out on the same sample and different displacement points were selected in each experiment. The displacement of the stationary skin and moving skin were analysed to determine the shear strain as mentioned in section3.3.3. In figure 5.1, it can be observed that all the 3 experiments gave almost the same curve. Therefore, it can be concluded that DIC through ARAMIS is reproducible.

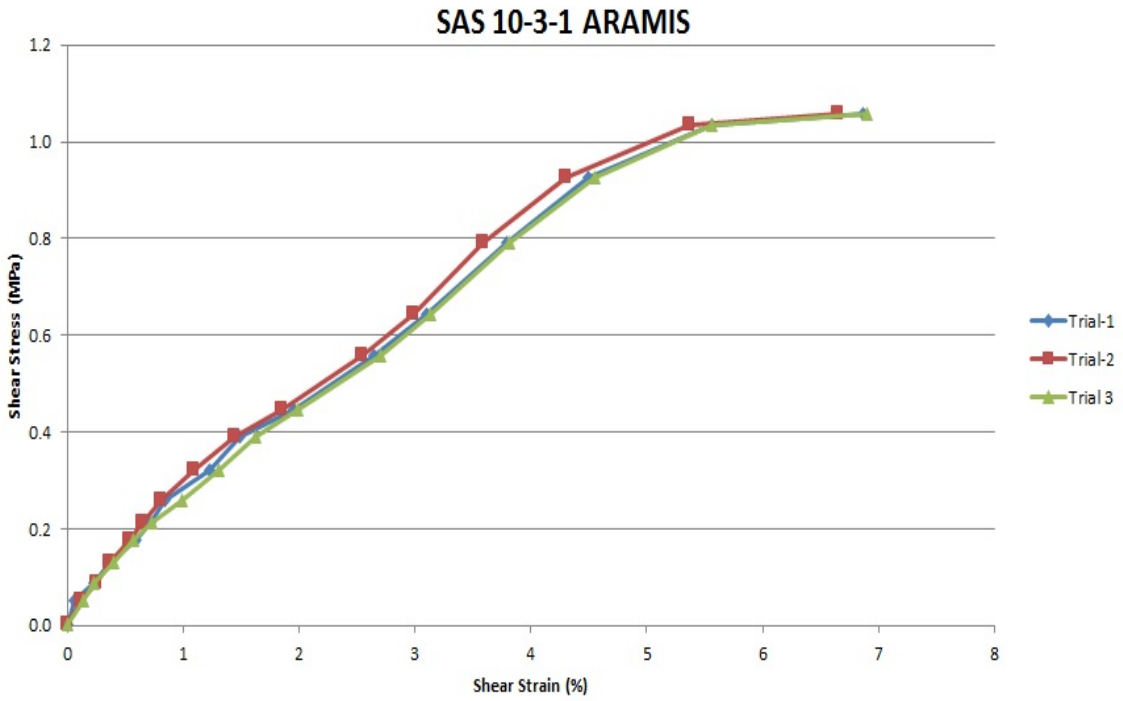

Figure 5.1: Reproducibility Proof

Second Experiment: To prove ARAMIS is reliable, an experiment was conducted where a steel block was stuck to the machine jig as shown in figure 5.2. The steel block was coated with the black speckle patter. The machine was given a displacement condition of 2mm/min without any application of load. The images were captured at an interval of 5 seconds and analysed in ARAMIS.

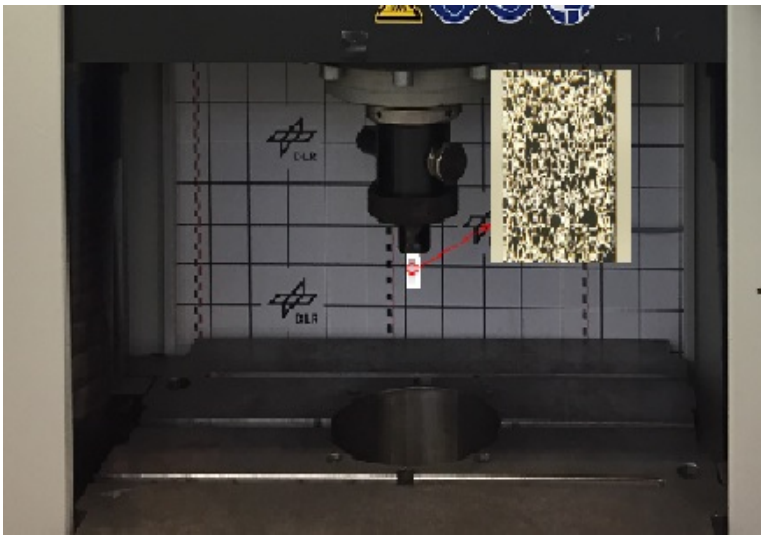

Figure 5.2: Experimental Setup for ARAMIS Reliability

The displacement of the steel block determined using ARAMIS was 1.70mm whereas the machine displacement was 1.66mm leading to a low error percentage of 2.4% between the machine and ARAMIS displacement. Therefore, it can be concluded that ARAMIS is a reliable method to measure the displacement of the coupon.

5.2 Shear Test

The shear stress is obtained from the shear test and the shear strain is determined through DIC (ARAMIS). The shear stress value from the test and shear strain value from the DIC are used to determine the shear modulus. 5 coupons are tested from each sample plate. All the coupons failed due to buckling and intra-laminar shear of the core as shown in figure 5.3. Therefore, the shear strength of different joining paste could not be determined and compared. The shear strain is determine by considering the complete free height of the core i.e. 13 mm. The joining meniscus is not considered for the shear strain calculation.

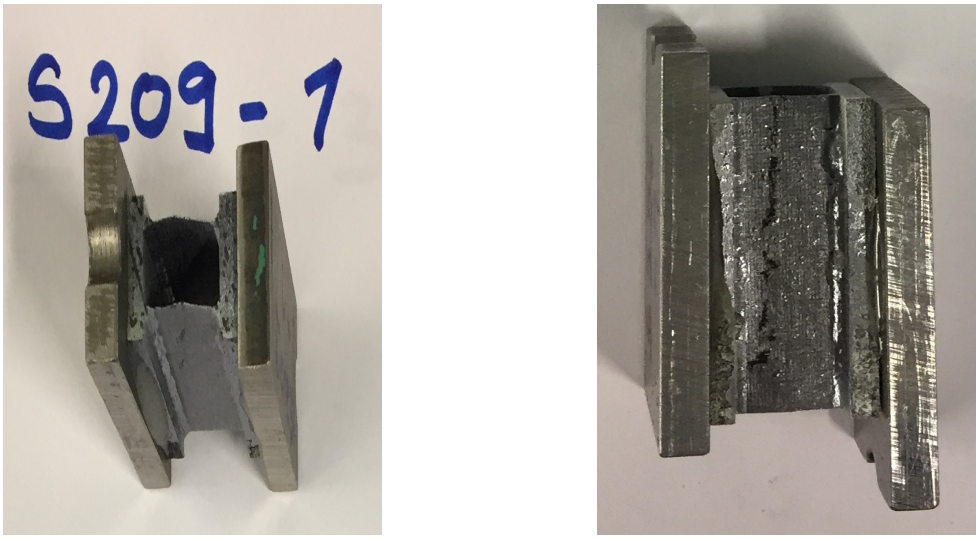

(a) (b)

Figure 5.3: Failure Modes of the Shear Coupon

1. S203

   The S203 sample plate was manufactured with reference phenolic joining paste i.e. the ratio of phenolic resin JK60 to PC40 carbon powder is 100:76 but the core was 0.7mm thick.

Coupon S203-2 was not bonded to the center of the jig. Hence, the load was not distributed uniformly which lead to the failure of only one web and a low shear stress of 22MPa compared to other coupons.

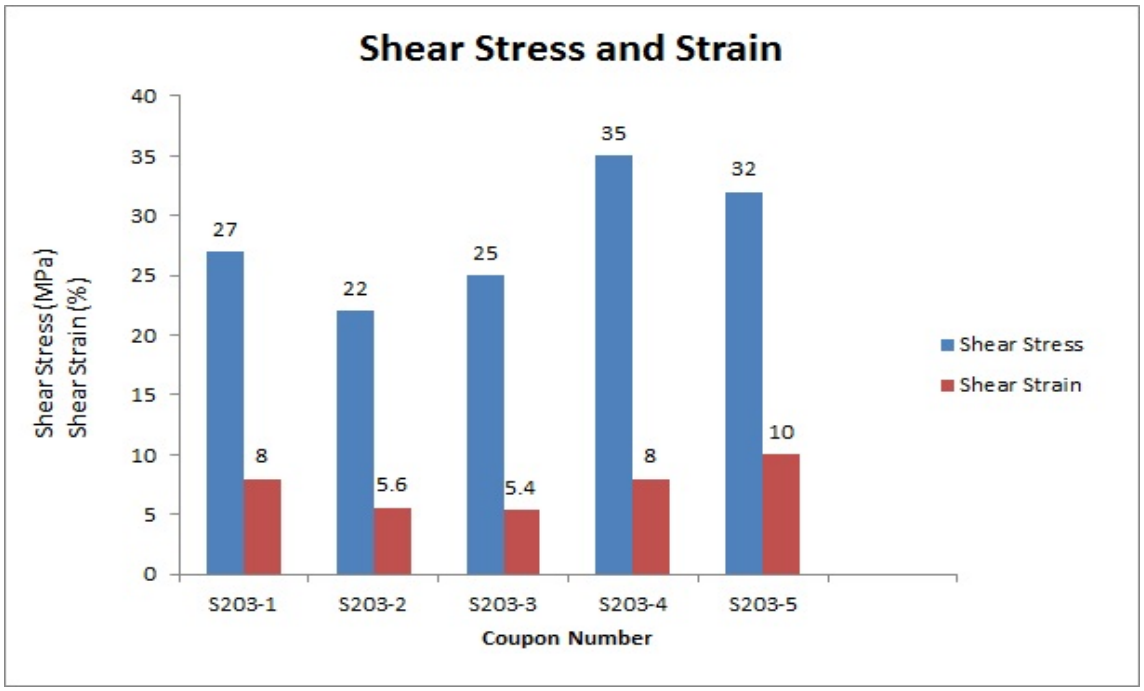

Figure 5.4: S203-Shear Stress and Strain

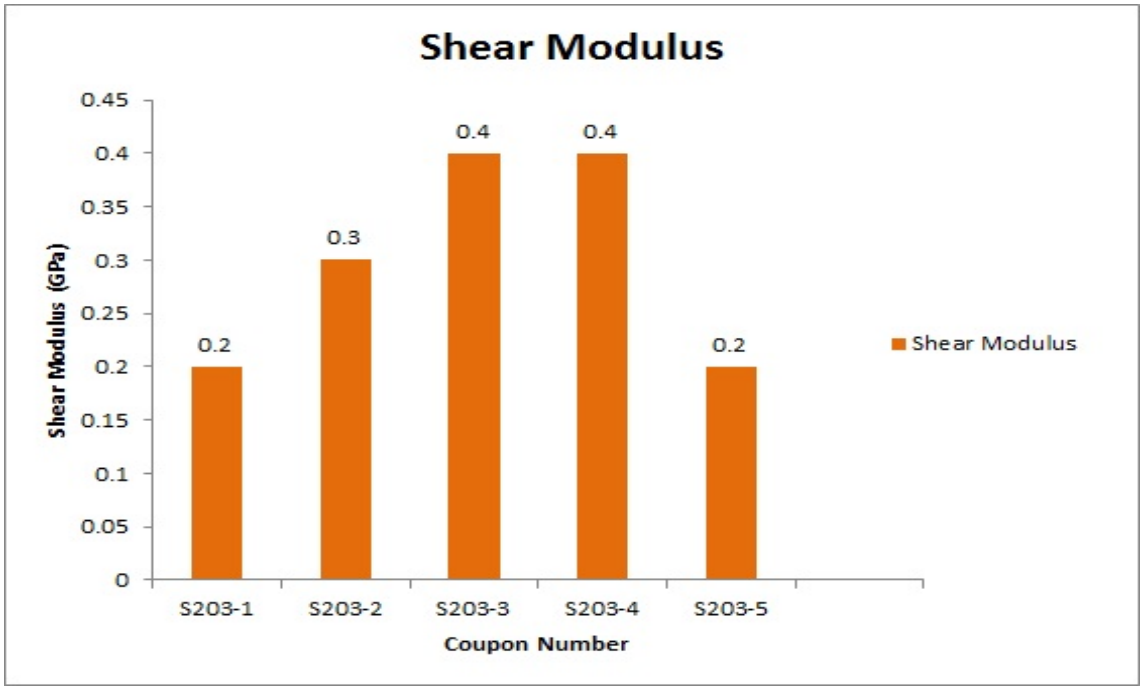

Figure 5.5: S203-Shear Modulus

2. S204

The S204 sample plate is manufactured using phenolic joining paste with a ratio of 100:68 i.e. 10% less PC40 than reference phenolic joining paste.

Coupon S204-4 was tilted while joining on to the jigs. Therefore, the load distribution on the coupon was not symmetric which lead to lower shear stress of 24MPa compared to other coupons.

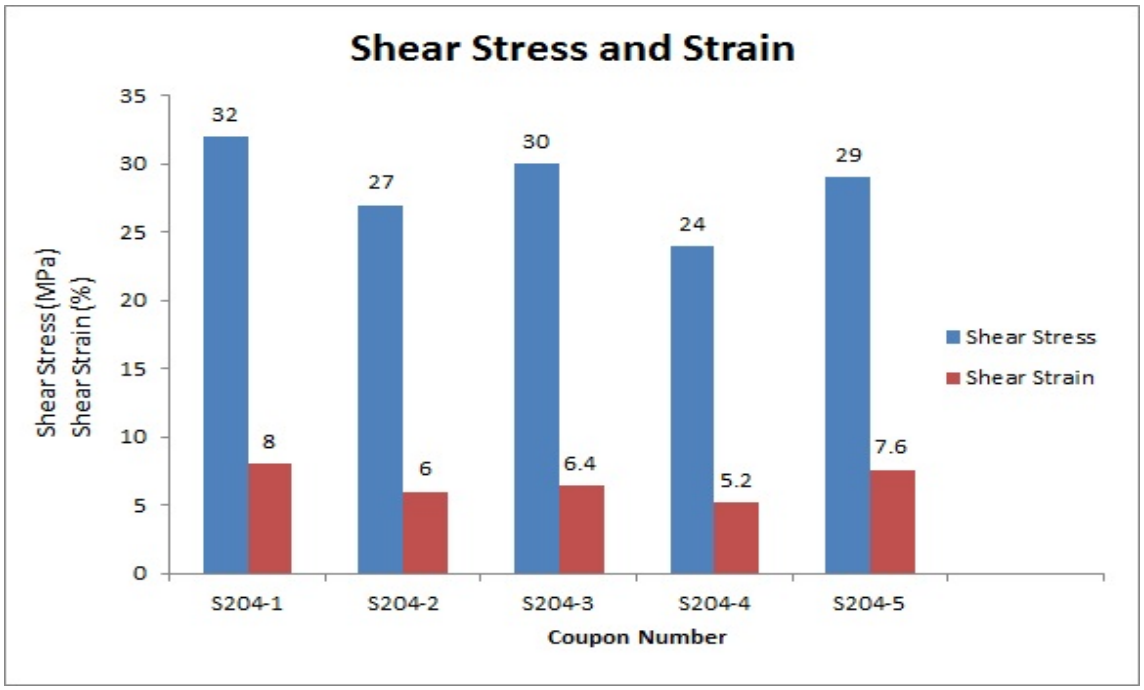

Figure 5.6: S204-Shear Stress and Strain

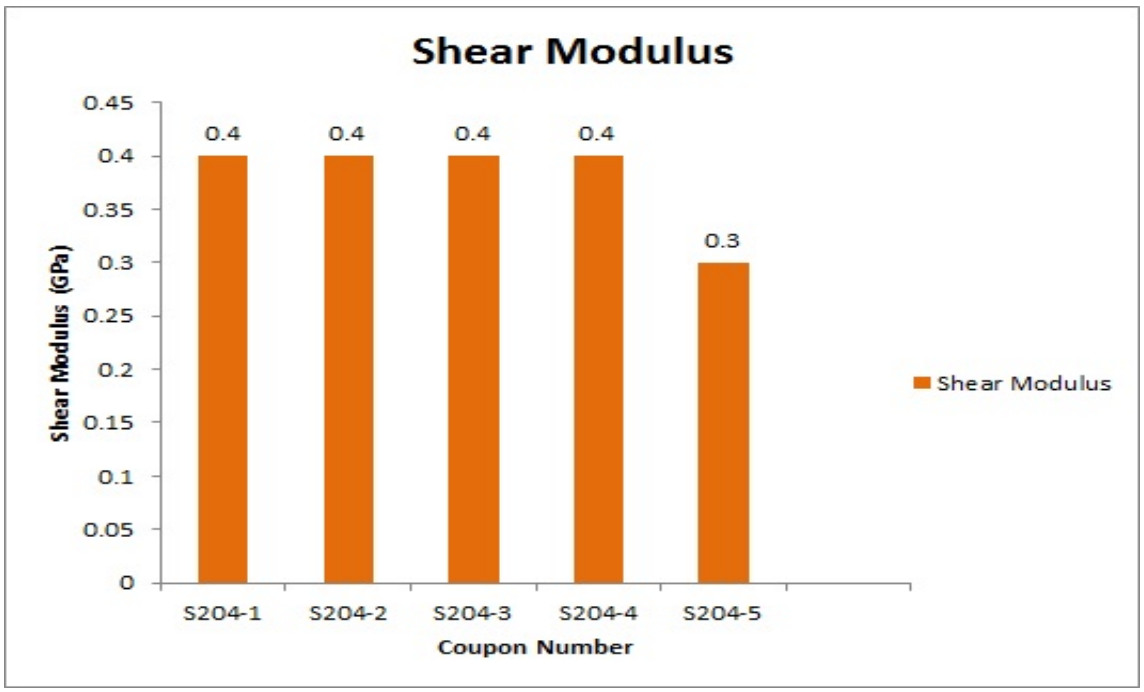

Figure 5.7: S204-Shear Modulus

3. S205

The S205 sample plate was manufacturing with phenolic joining paste. The ratio of JK60 phenolic resin to PC40 carbon powder was 100:60. The PC40 content is 20% lower than the reference phenolic joining paste.

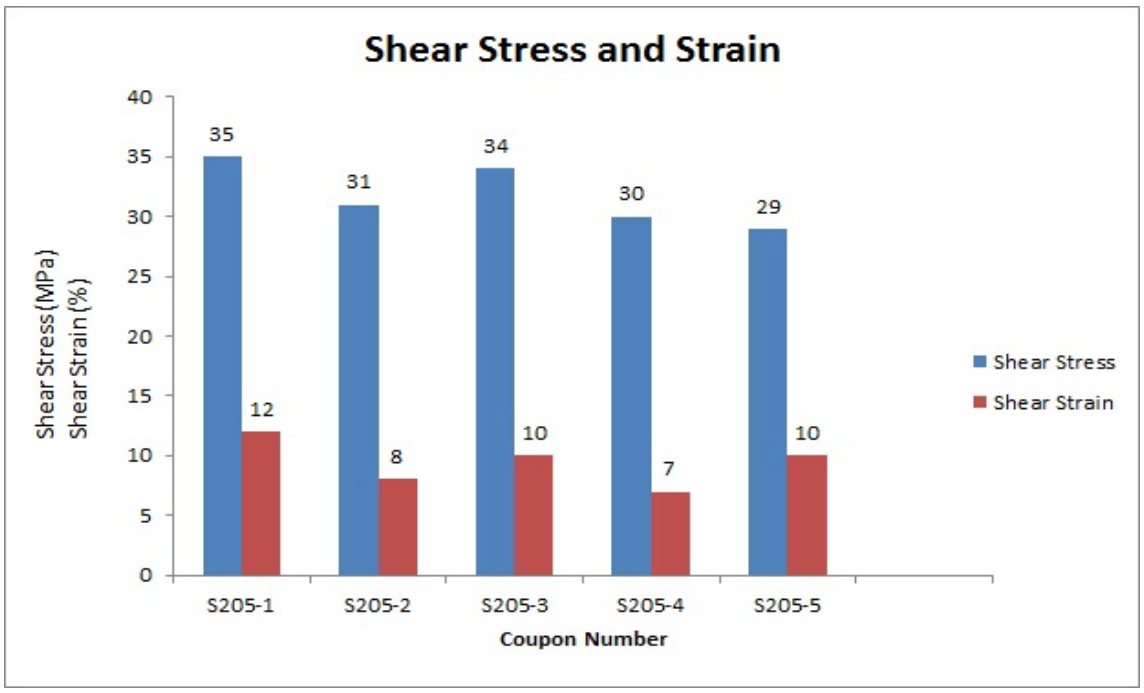

Figure 5.8: S205-Shear Stress and Strain

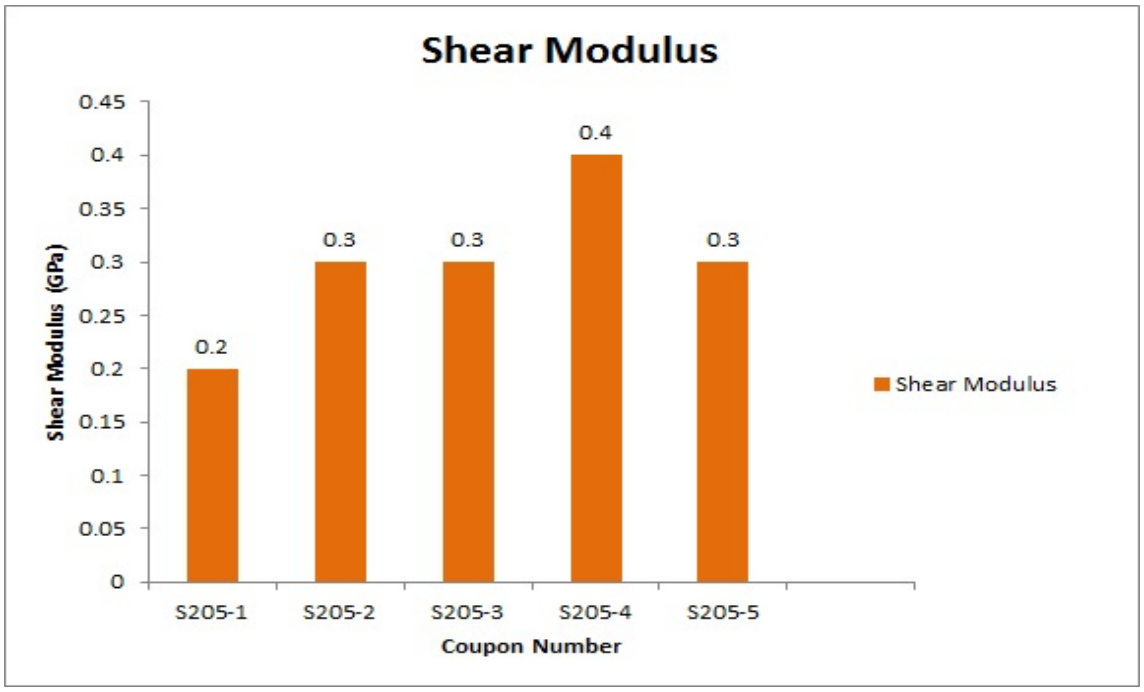

Figure 5.9: S205-Shear Modulus

4. S206

The S206 sample plate is manufactured using reference phenolic joining paste i.e. JK60:PC40 = 100:76. Coupon S206-5 broke while handling.

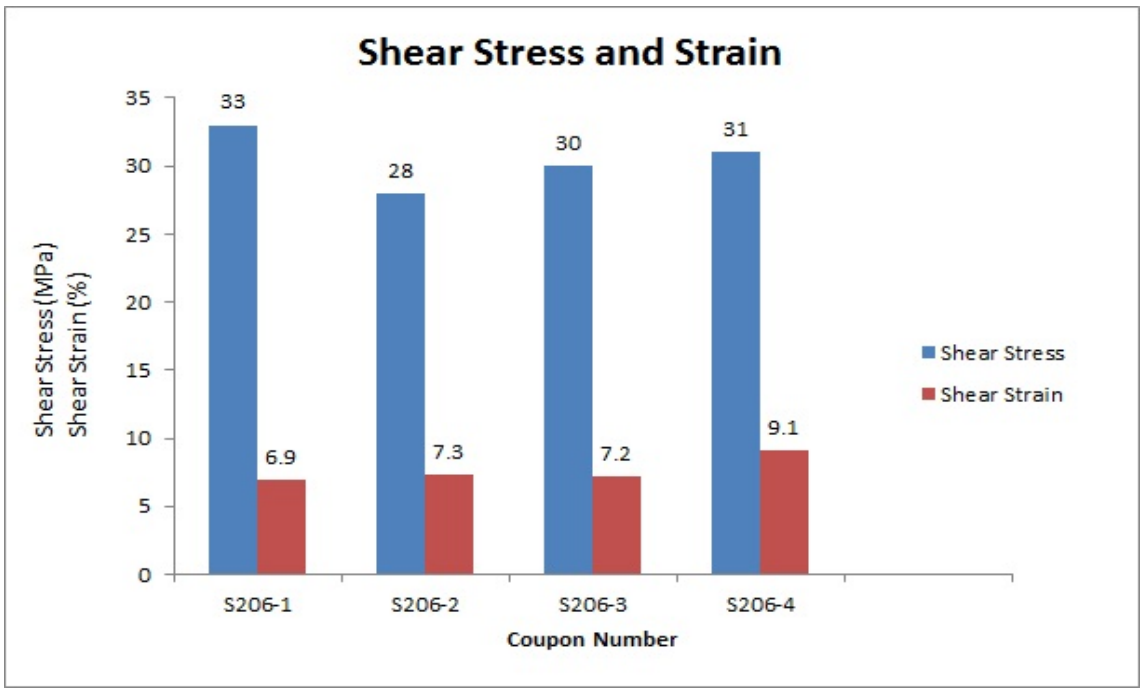

Figure 5.10: S206-Shear Stress and Strain

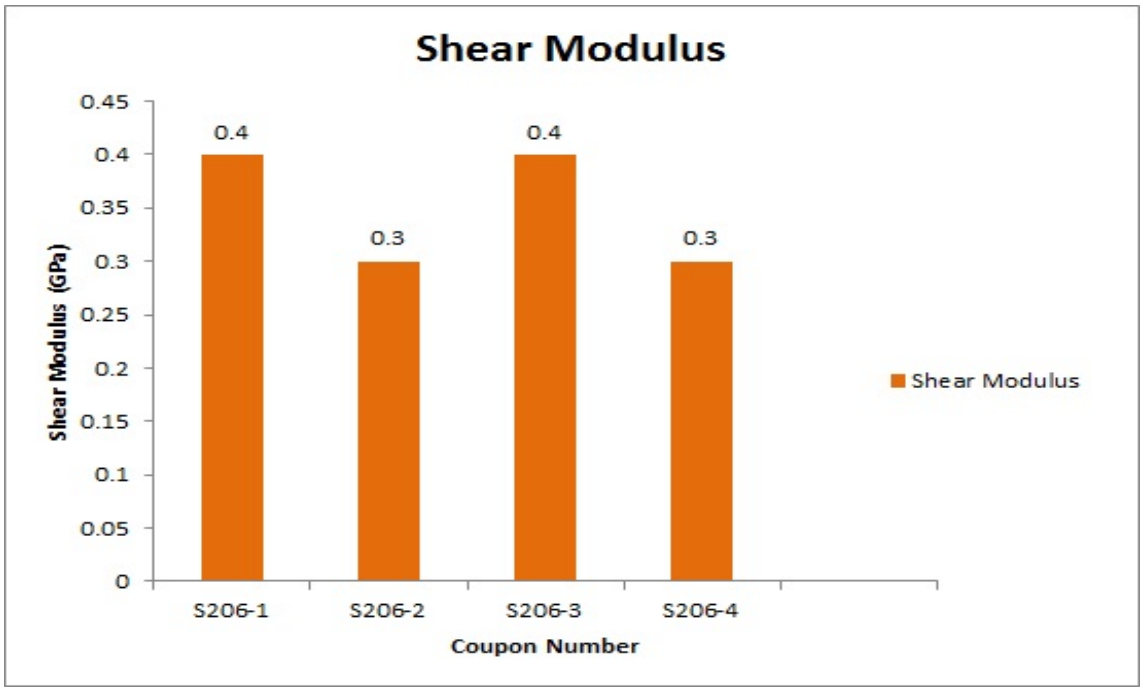

Figure 5.11: S206-Shear Modulus

5. S207

   The shear test was not performed on S207 coupons because the core was tilted during the siliconisation cycle as shown in figure5.12.

Figure 5.12: S207- Tilted Core

The core was tilted because the epoxy resin inside the joining paste begins to degrade at 300^0C which makes the structure unstable.

6. S208

   The S208 sample plate was manufactured using epoxy joining paste with a ratio of 100:108. The PC40 content was increase by 50% compared to S207. In order to maintain the viscosity at 18 Pa.s., 6 grams of acetone was added as a solvent.

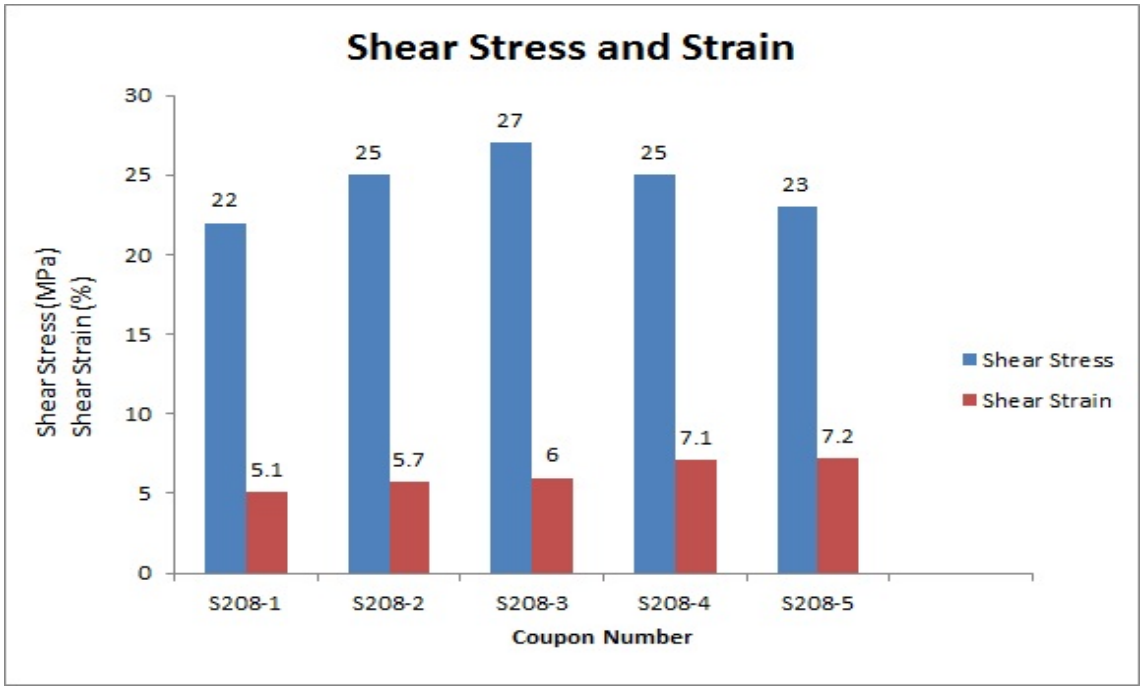

Figure 5.13: S208-Shear Stress and Strain

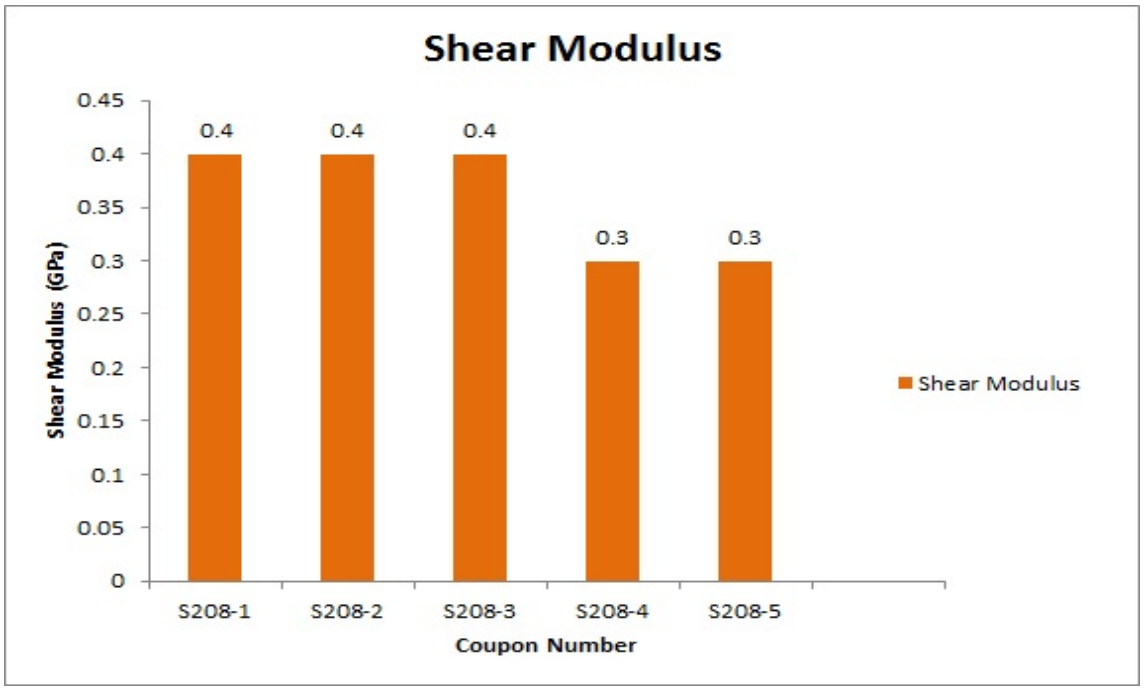

Figure 5.14: S208-Shear Modulus

7. S209

The S209 sample plate was manufactured using the combination of phenolic and epoxy joining paste. The coupon S209-5 was asymmetrically bonded to the jigs which resulted in the failure of a single web and shear stress of 23MPa compared to other coupons.

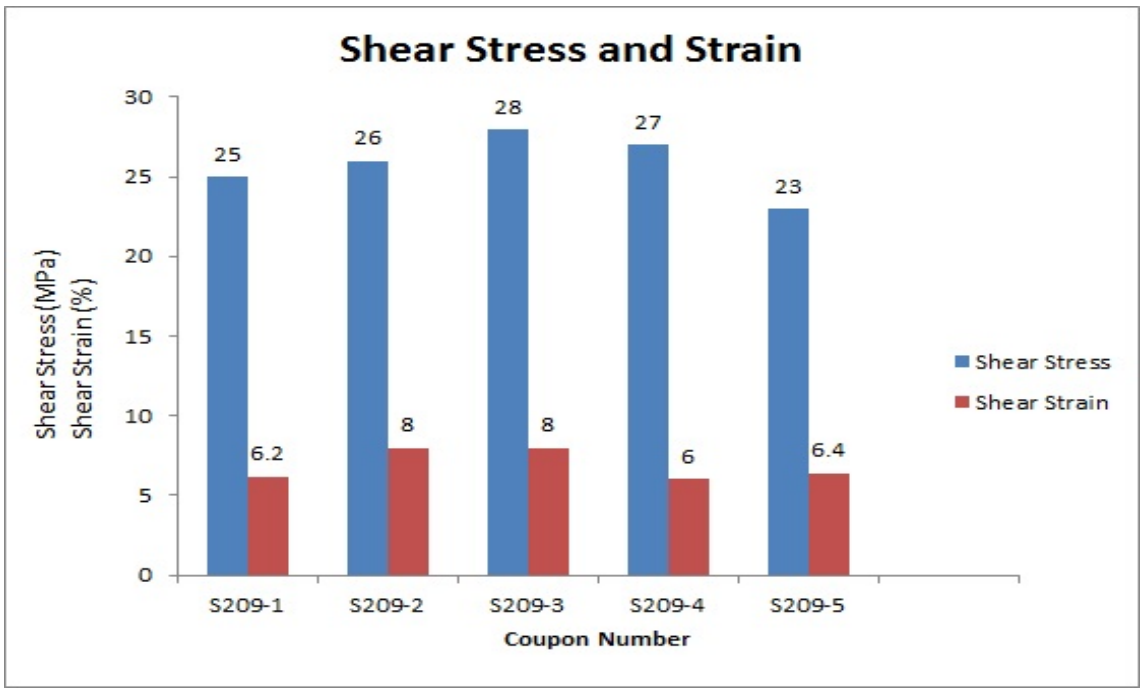

Figure 5.15: S209-Shear Stress and Strain

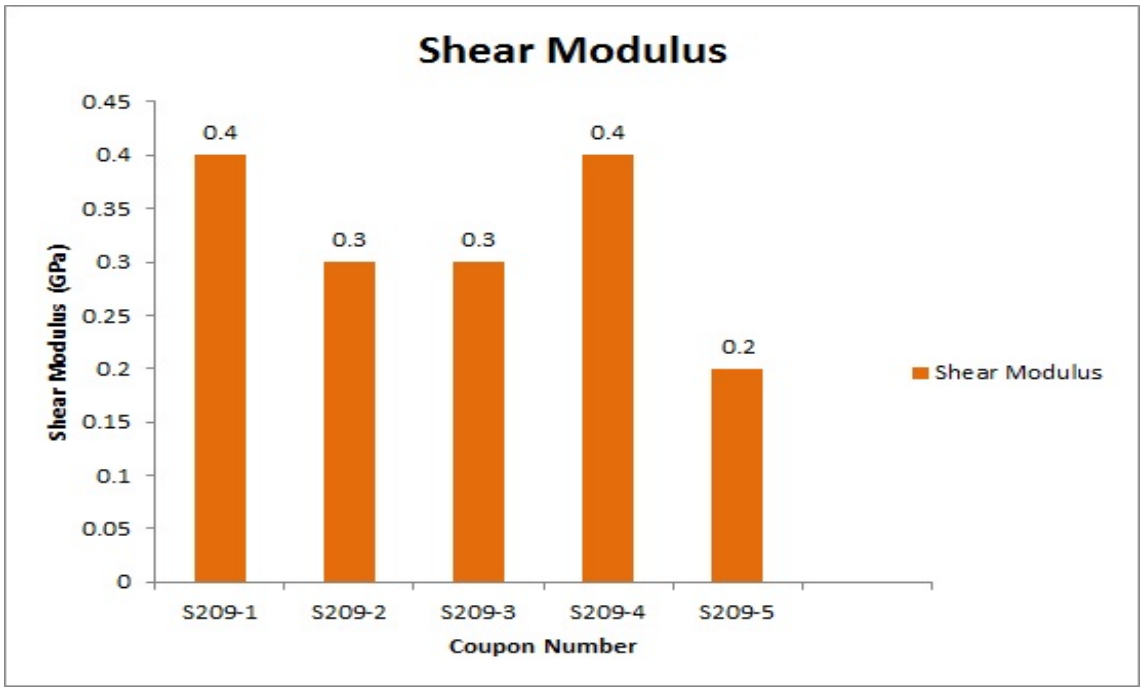

Figure 5.16: S209-Shear Modulus

8. S210

The S210 sample is manufactured with reference phenolic joining paste but with a gap of 0.15mm between the skin and core. The coupon S210-5 was not joined symmetrically to the jigs. Therefore, the load was not distributed uniformly on the coupon which lead to the failure of one web and a low shear stress of 20MPa compared to other coupons.

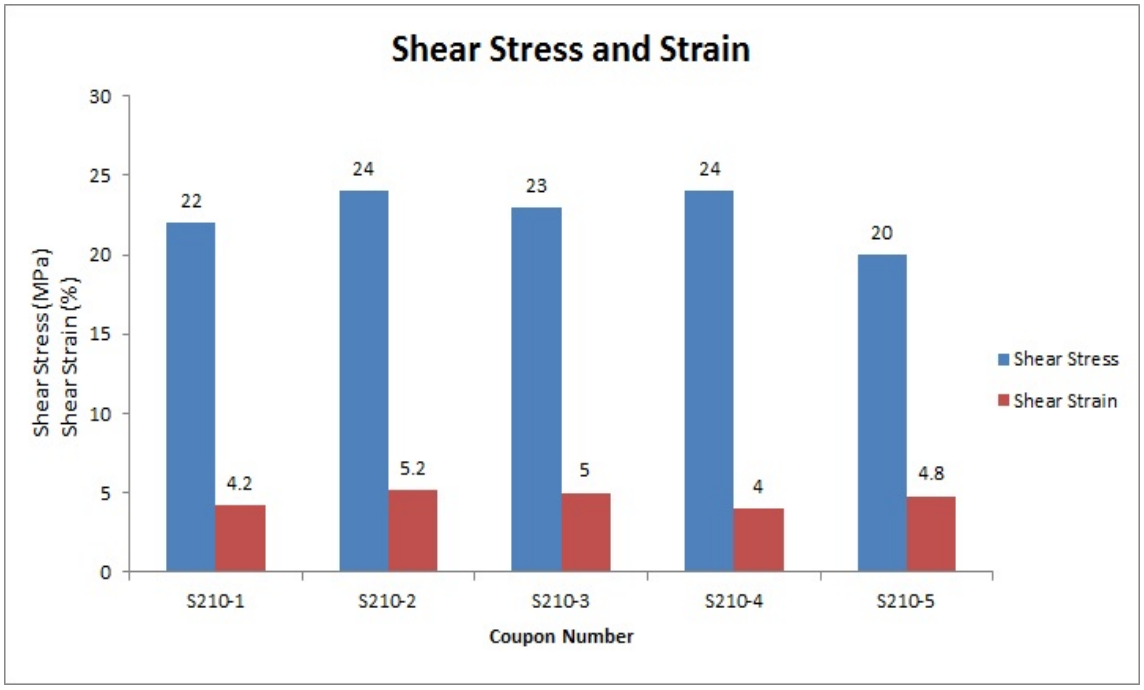

Figure 5.17: S210-Shear Stress and Strain

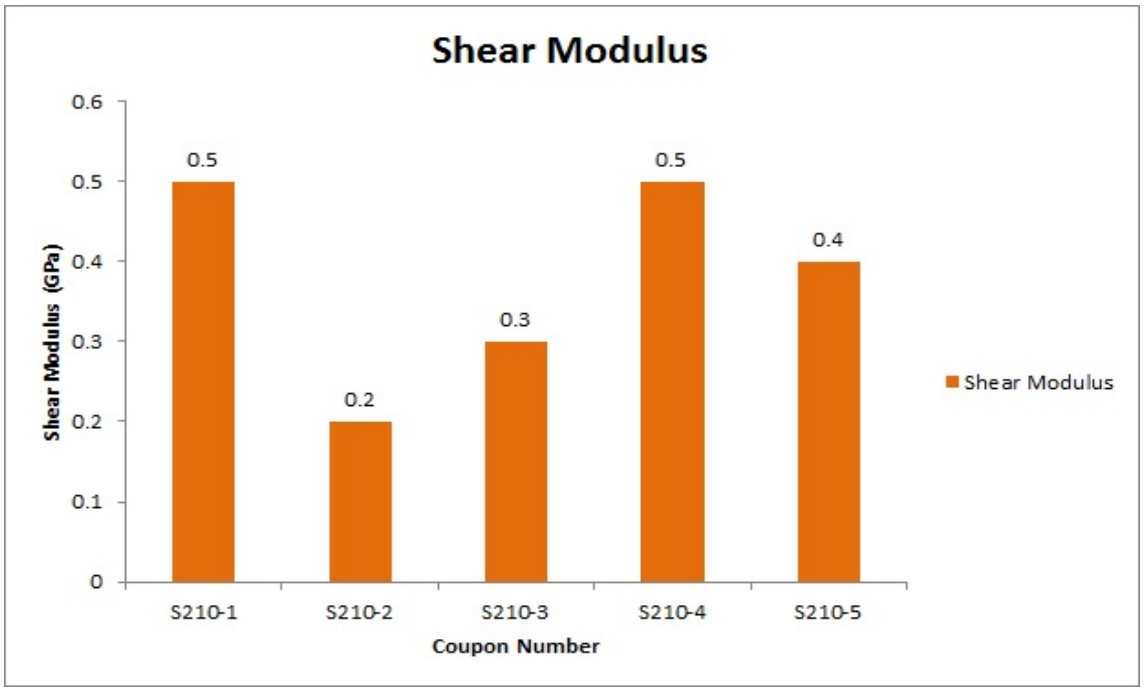

Figure 5.18: S210-Shear Modulus

9. Mean Shear Stress, Shear Strain and Shear Modulus

The failure occurred at the core, not in the joint. The mean value of the shear stress, strains and modulus from each sample plate are summarised below:

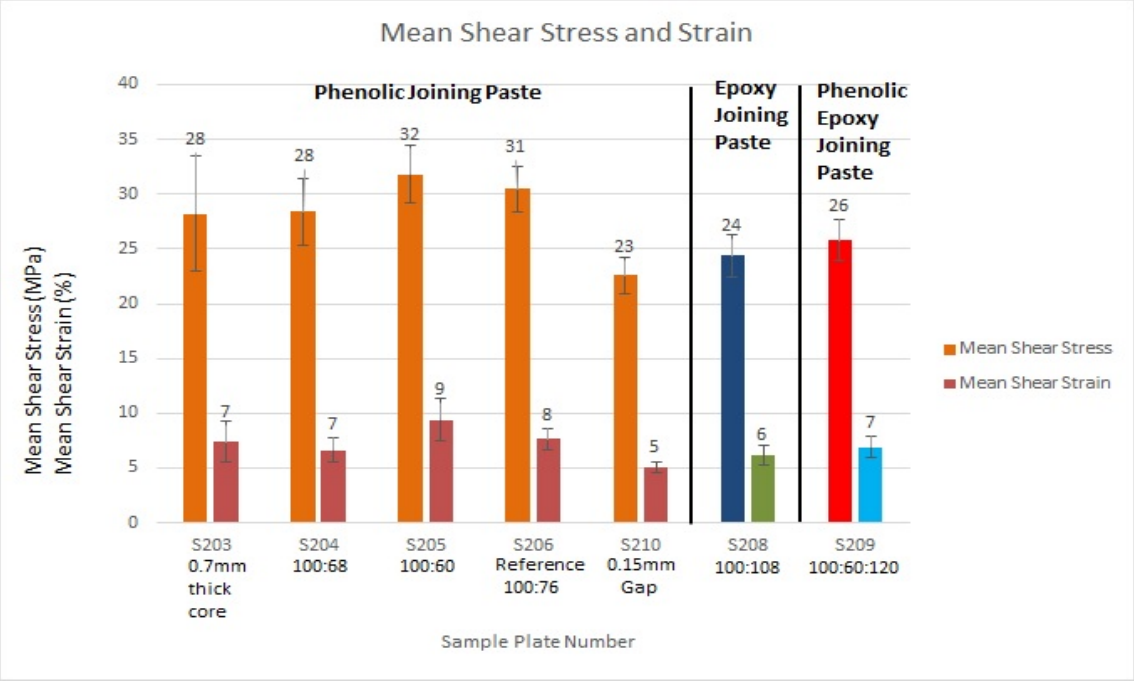

Figure 5.19: Mean Shear Stress and Strain

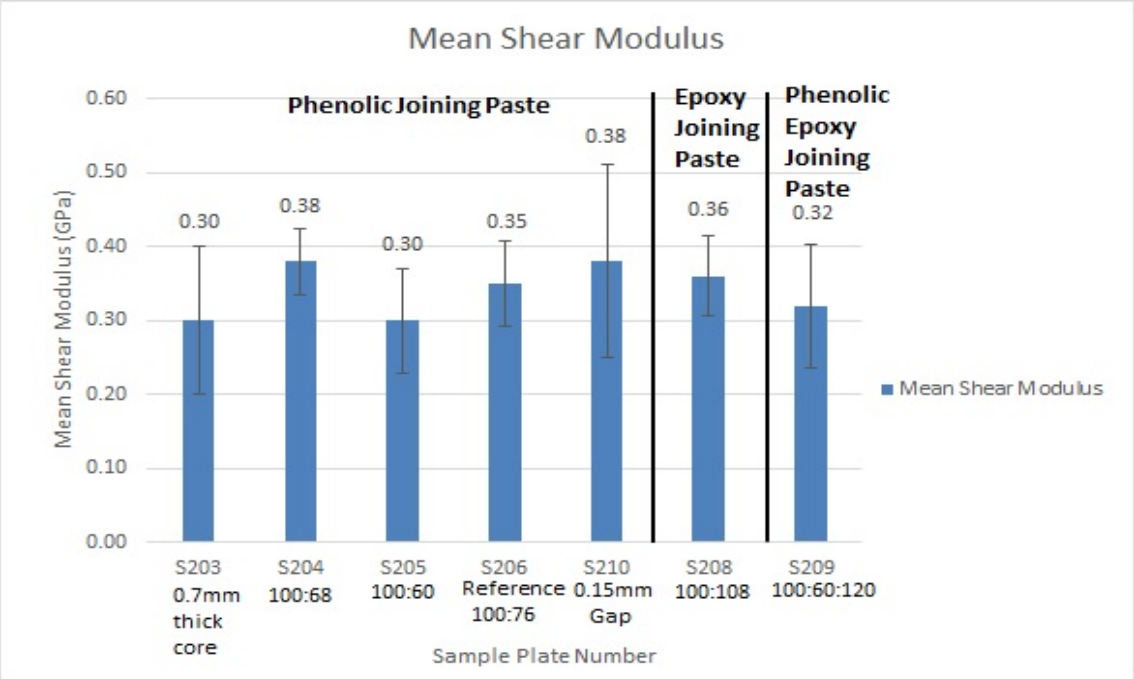

Figure 5.20: Mean Shear Modulus

Sample Plate Number		S203	S204	S205	S206	S208	S209	S210
Mean Shear Stress	**MPa**	28.20	28.40	31.80	30.50	24.40	25.80	23.0
Shear Stress Standard Deviation		5.26	3.05	2.59	2.08	1.95	1.92	1.48
Mean Shear Strain	**%**	7.40	6.64	9.40	7.63	6.22	6.92	5.06
Shear Strain Standard Deviation		1.92	1.15	1.95	1.00	0.91	1.00	1.42
Mean Shear Modulus	**GPa**	0.30	0.38	0.30	0.35	0.36	0.32	0.38
Shear Modulus Standard Deviation		0.10	0.04	0.07	0.06	0.05	0.08	0.13

Table 5.1: Mean Shear Stress, Shear Strain, Shear Modulus and Standard Deviation

From the figure 5.19 and 5.20, a range of shear stress, shear strain and shear modulus can be determined for the core:

Core Shear Stress = 23-32 MPa
Core Shear Strain = 5-9%
Core Shear Modulus = 0.3-0.4 GPa

5.3 Elemental Morphology

The Scanning Electron Microscope was used to analyse the presence of the elements in the joint after siliconisation. Ideally, the joint should contain only three elements i.e. carbon, silicon and silicon carbide. The presence of platinum can also be expected in a very small amount but it is due to the sputtering process which was done as a part of surface preparation for the SEM analysis. The section 5.2 mentions the colour difference between the carbon, silicon and silicon carbide. In general, the colour representation in SEM is assigned based on the atomic number of the element i.e. the element with the lowest atomic number will have the darkest colour and element with highest atomic number will have the brightest colour.

Colour	Element
Black	Carbon
Grey	Silicon Carbide
White	Silicon

Table 5.2: Representation of Colours

Histogram technique was used to quantify each element in the joining paste. The rule of mixture can be used to determine the properties of the joint based on the percentages of the elements present. For example,

Youngs Modulus of Si (E_{Si}) = x
Youngs Modulus of C (E_C) = y
Youngs Modulus of SiC (E_{SiC}) = z

% of Residual C = 80%
% of SiC = 15%
% of Si = 5%
Therefore,

$$E_{joint} = 0.05 \times x + 0.8 \times y + 0.15 \times z$$

The joining meniscus can be simulated so that the finite element model is close to the real structure. The properties of different joining paste can be implemented into the model and their effect can be analysed.

The element morphology and element content for each joining paste variation is mentioned below:

1. **S203 - 0.7mm thick core**
   The reference phenolic joining paste configuration i.e. 100:76 was used for manufacturing the sample. Since the core has a thickness greater than 0.3mm, the amount of silicon infiltrated was changed from 200% to 45% for the core.

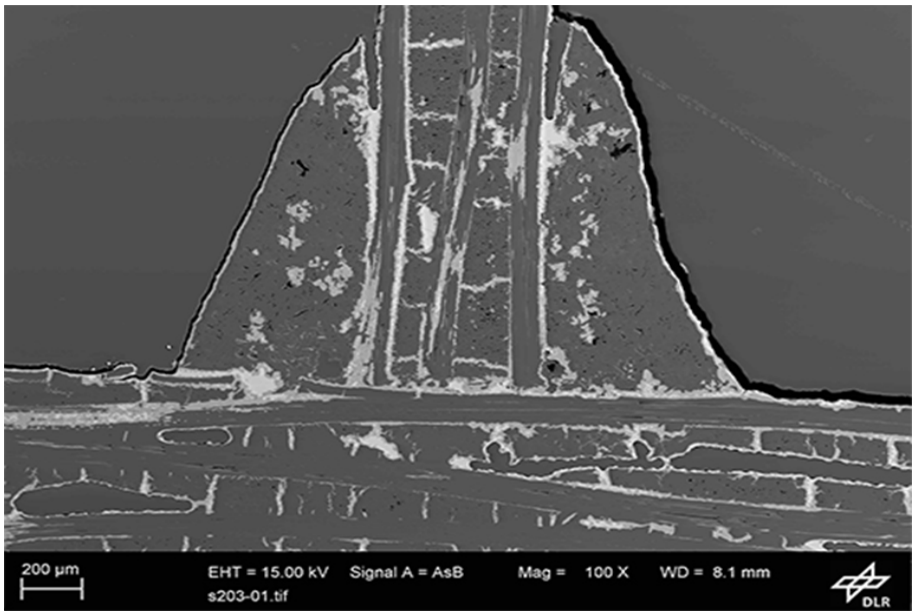

Figure 5.21: S203

   % of Residual C = 80%

   % of SiC = 15%

   % of Si = 5%

2. **S204 - Phenolic Joining Paste (100:68)**

   The PC40 content was reduced by 10% compared to the reference phenolic joining paste so that less than 50% residual carbon is obtained.

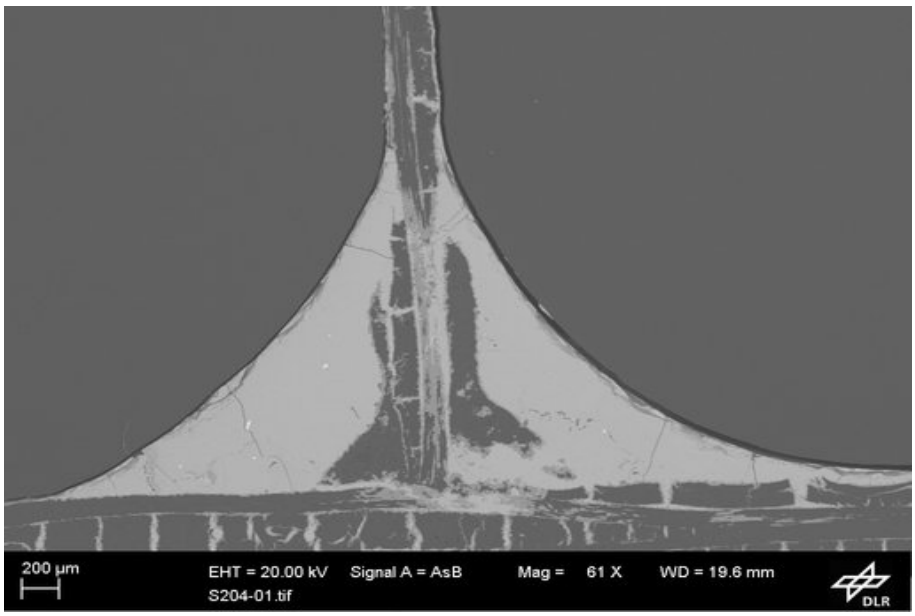

Figure 5.22: S204

% of Residual C = 20%

% of SiC = 10%

% of Si = 70%

3. **S205 - Phenolic Joining Paste (100:60)**

The PC40 content was reduced by 20% compared to the reference phenolic joining paste so that residual carbon is reduced in order to make the joint thermally stable at high temperature.

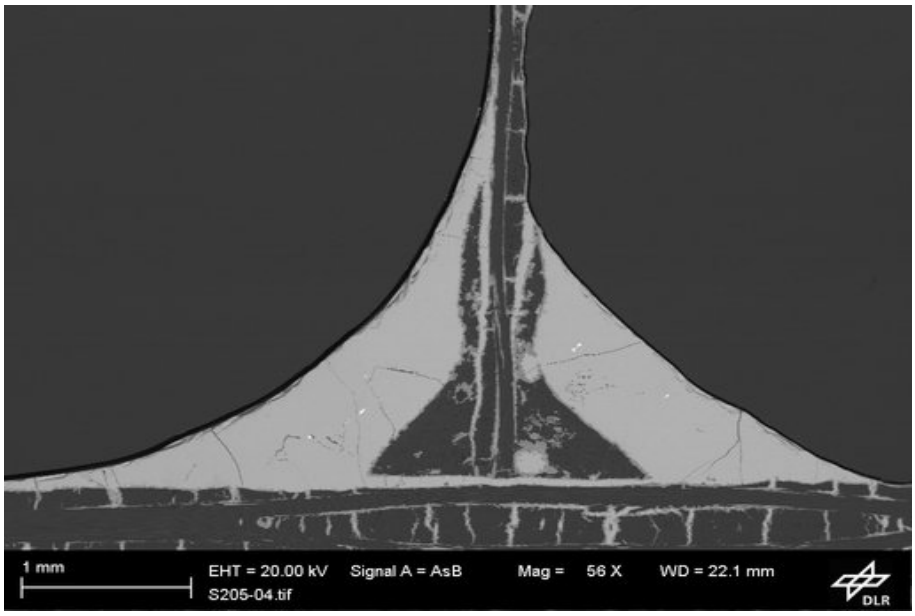

Figure 5.23: S205

% of Residual C = 23%

% of SiC = 8%

% of Si =69%

4. **S206 - Reference Phenolic Joining Paste (100:76)**

The elemental morphoogy of the other samples can be compared to this sample as it is considered to be the reference joining paste which is stable upto 1500^0C [8].

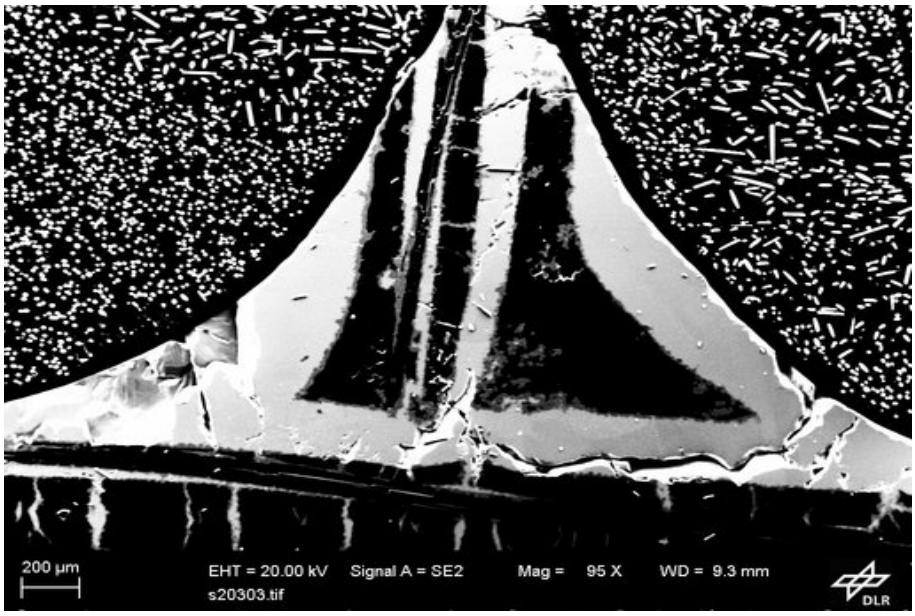

Figure 5.24: S206

% of Residual C = 40%

% of SiC = 9%

% of Si = 51%

5. **S208 - Epoxy Joining Paste (100:108)**

PC40 content is increased by 50% compared to S207 sample so that more residual carbon can be obtained which will assist to increase the shear strength.

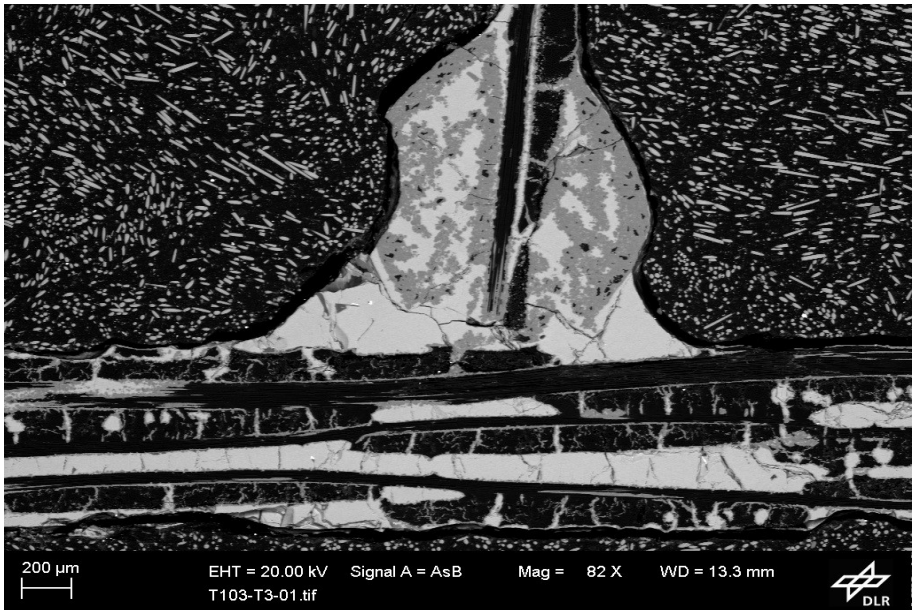

Figure 5.25: S208

% of Residual C = 3%

% of SiC = 77%

% of Si = 20%

6. **S209 - Phenolic Epoxy Joining Paste (100:60:120)**

The configuration of this paste was selected such that the elemental morphology can be compared to the reference phenolic joining paste i.e. S206

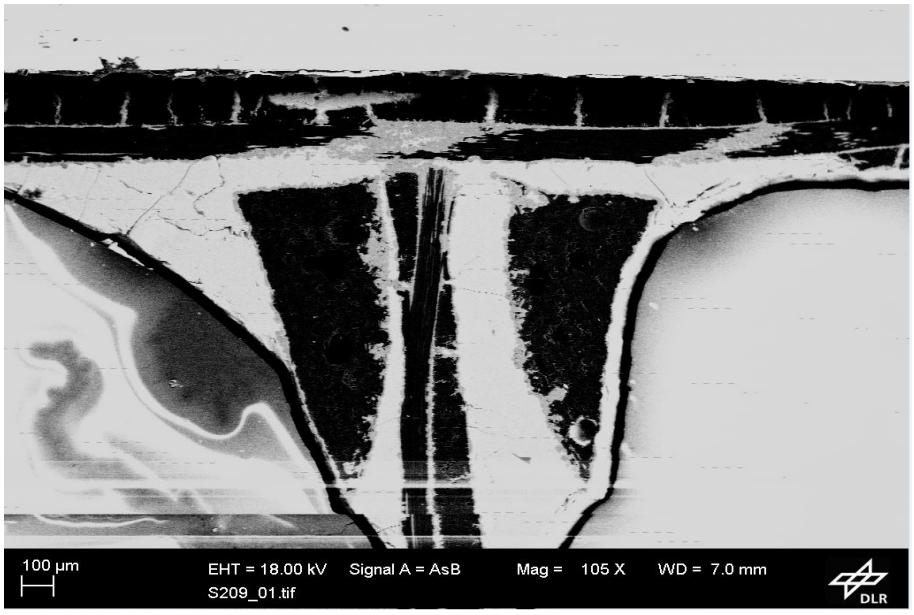

Figure 5.26: S209

% of Residual C = 43%

% of SiC = 10%

% of Si = 47%

7. **S210 - Gap of 0.15mm between the skin and core**

   Reference phenolic joining paste configuration i.e. 100:76 is used for manufacturing the sample. It can be observed that the gap between the skin and core is filled with silicon

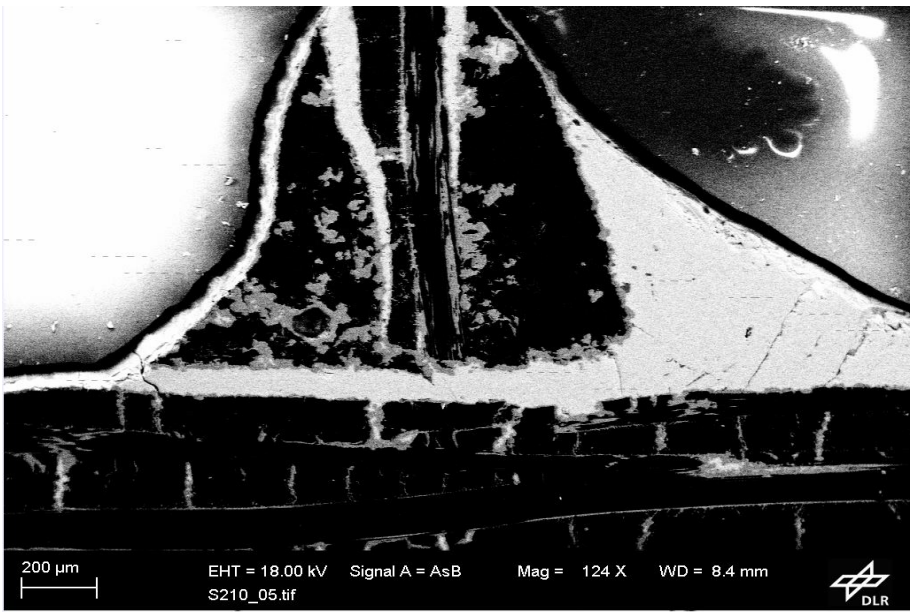

Figure 5.27: S210

% of Residual C = 45%

% of SiC = 9%

% of Si = 46%

5.4 Overview of samples

1. S203

   The sample was manufactured with a thicker core of 0.7mm (3 layer)so that the failure can occur at the joint. The silicon infiltration for the core was reduced to 45% from 200% as the core was thicker. The infiltrated silicon was not enough as it can be seen in figure 5.21 that residual carbon content is 80%. Even though the core was thicker compared to the other samples but the shear stress was 28 MPa. This is due to the low silicon infiltration.

2. S204

   The carbon content was reduced by 10% compared to reference phenolic joining paste so that less residual carbon is obtained. In figure 5.22, it can be observed that the carbon content is reduced but the silicon content is excess. Excess silicon infiltration makes the joint brittle. It can be said that the joint can withstand minimum shear stress of 28 MPa.

3. S205

   The carbon content was reduced further to 20% compared to the reference phenolic joining paste so that the influence of reduced PC40 content on the shear stress can be compared to the reference phenolic joining paste. The elemental morphology of S205 was similar to S204 but the shear strength of the joint could not be compared because the failure occurred at the core. As mentioned above, it can be said that the joint can withstand a minimum shear stress of 32 MPa.

4. S206

The shear strength of the reference phenolic joining paste could not be determined as the coupons failed at the core. The elemental morphology shows excess residual carbon which makes the joint unstable at high temperature ($> 1500^0C$).

5. S207

   The epoxy joining paste assists in achieving the goal of obtaining more than 50% SiC in the joint which makes the joint thermally stable but residual stresses were generated during siliconisation because of the degradation of epoxy resin at 300^0C. The degradation of the resin lead to severe shrinkage of the joining paste and finally to the tilting of the core. During the tensile test, it was observed that tensile strength of epoxy joining paste is 10 MPa lower than reference phenolic joining paste. All these factors restricted the use of epoxy joining paste for further research.

6. S208

   In order to increase the strength of the epoxy joining paste, the residual carbon content needed to be increased. Thus, the PC40 content was increased by 50% compared to S207. The viscosity was maintained by adding 6g of acetone which increased the curing time by 12 hours. The increase in curing time extends the manufacturing time which is not beneficial for mass production.

7. S209

   The combination of phenolic joining paste and epoxy joining paste resulted in an innovative solution for bonding the C/C structures. The major advantage of phenolic epoxy joining paste is the room temperature curing which takes only 6 hours. Another advantage is that after curing the joining paste is less stiff but after tempering the joining paste for 2 hours at 220^0C, the joining paste becomes rigid. Therefore, this property opens the gates for joining curved structures. The configuration of the phenolic epoxy joining paste was selected such that it can be compared to the reference phenolic joining paste and it can be observed from figure 5.26 that the proportion of the elements is similar to reference phenolic joining paste i.e. figure 5.24. Although the shear strength could not be compared as the failure occurred in the core but the goal of achieving more than 50% SiC in the joint can be established by altering the epoxy content in the mixture as it is observed from figure 5.25 that epoxy joining paste transforms most of the carbon into SiC.

8. S210

   The gap analysis was performed to analyse the effect of the manufactruing tolerances on the shear stress but since the failure did not occur at the joint, it can be concluded that the gap between the skin and the core does not have any influence on the shear strength of the joint. This is due to the infiltration of silicon in the gap as observed in figure 5.27 which strengthens the structure.

The main goal of the thesis was to achieve more than 50% SiC in the joint so the joint becomes thermally stable at high temperature ($> 1500^0C$) along with a shear strength greater than 11 MPa.

- Due to the failure occurring at the core, the shear strength of joining paste could not be determined. It can be concluded that the joining pastes can withstand a minimum shear stress ranging from 23 MPa - 32 MPa.

- The epoxy joining paste used for sample S207 does satisfy the goal of achieving more than 50% SiC but it becomes unstable at 300^0C due to the resin degradation.

- The epoxy joining paste used in sample S208 also satisfies the aim of achieving more than 50% SiC at the joint but the curing time is too long compared to the reference phenolic joining paste configuration. Another aim was to obtain more residual carbon compared to figure 3.12b but the residual carbon content is not increased even after adding 50% more PC40 powder.

- The phenolic epoxy joining paste configuration shows elemetal morphology similar to reference phenolic joining paste because the mixture was optimised for the comparison. The configuration of the mixture can be altered to obtain more than 50% SiC content at the joint by increasing the amount of epoxy resin in the paste. From sample S208 it is evident that epoxy joining paste

transforms almost all the carbon into SiC. Hence, phenolic epoxy joining paste proves to be the best fit for the manufacturing of C/C-SiC sandwich structure with grid core.

6 *Conclusion and Recommendation*

The C/C-SiC sandwich structures are opening possibilities for application in highly stiff and thermally stable satellite structures. At DLR, the initial phase towards the development of C/C-SiC sandwich structures using LSI technique is underway. The joining of the skin and the core components. Amongst the existing manufacturing processes for C/C-SiC structures, LSI technique is used at DLR because it is cost efficient, time efficient and better quality of end product is obtained. The existing manufacturing process for C/C-SiC sandwich structures using LSI technique is improved by degassing the joining pastes, using a mould with a defined depth such that the thickness of the joining layer is homogeneous on the core and by using different percentage of silicon infiltration for the skin (3mm thick) and the core (0.3mm thick) assisted in giving more uniform joining meniscus. The experimental setup is improved to give more uniform strain distribution in the structure which was helpful for DIC (ARAMIS). The reliability and reproducibility of ARAMIS was proved and the process to determine shear strain for the thin walled shear coupon is explained so that accurate results are obtained. The shear strength of the different joining pastes could not be determined and compared because all the coupons failed at the core. The mode of failure was buckling and intra-laminar shear. Since the coupons failed at the core, it can be concluded that the joining paste can withstand a minimum shear stress of 23-32 MPa. A range of core properties were stated as shown below:

- Core Shear Stress = 23-32 MPa
- Core Shear Strain = 5-9%
- Core Shear Modulus = 0.3-0.4 GPa

The goal of obtaining more than 50% SiC in the joint was achieved by epoxy joining paste but the unstable behaviour of epoxy at 300^0C and extended curing time makes it a secondary option for high temperature stable joint. The phenolic epoxy joining paste can be altered to obtain 50% SiC in the joint which is the most promising option for faster room temperature curing and if researched further can mark a breakthrough in the field of CMC's.

Recommendations:

1. The existing test method should be improved so that the line of action is identical for the two opposite forces at Jig 1 and Jig 2. This will help in reducing the moment and achieving more shear dominated behaviour.

2. Different combinations of phenolic epoxy joining paste should be experimented to achieve the goal of more than 50% SiC at the joint. The amount of epoxy resin can be increased so that the transformation of carbon to SiC is increased.

3. The rule of mixture can be applied to the element percentages mention in section 5.3 to obtain the properties of the joint which can be used for Finite Element Analysis of shear coupon or C/C-SiC sandwich structure with the joining meniscus.

4. A standard testing method can assist in comparing shear strain measuring techniques. For example, the shear strain value from DIC can be compared with the shear strain obtained by the method mentioned in the standard.

5. Silicon infiltration needs to be refined so that excess silicon is not infiltrated as it adds to the weight of the structures as well as makes the joint brittle.

Bibliography

[1] W. Krenkel, "Carbon fibre reinforced silicon carbide composites (C/SiC, C/C-SiC)," *Handb. Ceram. Compos.*, pp. 117–148, 2005. [Online]. Available: `http://link.springer.com/chapter/10.1007/0-387-23986-3%7B%5C_%7D6`.

[2] B. Heidenreich, "Carbon Fibre Reinforced SiC Materials Based on Melt Infiltration," *Proc. 6th Int. Conferance High Temp. Ceram. matrix Compos.*, pp. 2–7, 2007.

[3] W. Krenkel, *Ceramic matrix composites: Fiber reinforced ceramics and their applications*, 2nd Edition. Wiley, 2008.

[4] C. Kassapoglou, *Design and analysis of composite structures: With applications to aerospace structures*, 2nd Edition. Wiley, 2013.

[5] A. Petras, "Design of sandwich structures," *Composite Structures*, 1998.

[6] N. Gottschalk, "Entwicklung von c/c-sic sandwichbauweisen auf der basis von faltstrukturen (unpublished)," 2014.

[7] R.V.Shirke, "C/c-sic sandwich structure based on grid type core (unpublished)," 2015.

[8] N. M. Walter Krenkel,T. Henke, "Insitu Joined Cmc," *Key Eng. Mater.*, pp. 127–131, 1997.

[9] S. R. R. Domenick E. Cagliostro, US4824711 A.

[10] H. W. Xiao-zhou Wang Jun Wang, "Preparation and performance of a heat-resistant organic adhesive obtained via a liquid sic precursor," vol. 35, pp. 17–20, 2012.

[11] W. H.L.Fan F.H. Meng, "Sandwich panel with kagome lattice cores reinforced by carbon fibers," *Composite structures*, pp. 533–539, 2006.

[12] D. Han and S. W. Tsai, "Interlocked composite grids design and manufacturing," 2002.

[13] Y. J.Xiaong L.Ma and S.Pan, "Bending response of carbon fiber composite sandwich beams with three dimensional honeycomb cores," 2014.

[14] V. N. V.Zh.Shemet A.P. Pomytkin, "High-temperature oxidation behaviour of carbon materials in air," *Carbon*, vol. 31, pp. 1–6, 1992.

[15] W. J. Miller, "High temperature oxidation of silicon carbide," 1972.

[16] D. Hartz, D. Erickson, W. Hopkins, and C. Pederson, *Composite honeycomb sandwich structure*, US Patent 5,604,010, Feb. 1997. [Online]. Available: `https://www.google.com/patents/US5604010`.

[17] V. A. Amir Fathi Jan-Hendrik Keller, "Full-field shear analyses of sandwich core materials using digital image correlation (dic)," pp. 156–166, 2014.

[18] A. K. A. Gardziella L.A. Pilato, "Phenolic resins: Chemistry, applications, standardization, safety and ecology," p. 119, 2013.